Intercomparison of extensional flow characterization techniques for polymer melts: tensile stretching and converging flow methods

M. Rides, C.R.G. Allen and
S. Chakravorty

April 1999

NPL Report CMMT(A)171

CMMT(A)171
April 1999

Intercomparison of extensional flow characterization techniques for polymer melts: tensile stretching and converging flow methods

M. Rides, C.R.G. Allen and S. Chakravorty
Centre for Materials Measurement and Technology
National Physical Laboratory
Teddington, Middlesex
United Kingdom
TW11 0LW

ABSTRACT

Although extensional flow properties of polymer melts play an important role in their behaviour in processing, these properties are rarely characterised compared with that of their shear flow properties. Furthermore, the measurement of extensional flow behaviour is more complex than that of shear flow behaviour, and the variation in data that is likely to be obtained when using different instruments and techniques is not established. An intercomparison of extensional flow characterization techniques for polymer melts was organised to assess the variation in data obtained when using different instruments and methods. The results of this intercomparison are reported.

The methods used in the intercomparison were principally tensile stretching and converging flow methods, although fibre spinning and a flow visualisation method were also included. A high density polyethylene that was stable at 190 °C for in excess of two hours was used as the intercomparison material. Measurements were made at 150 °C and 190 °C.

For tensile stretching methods the variation in extensional stress growth coefficient values was estimated to be up to ± 60%. The variation in peak extensional stress growth coefficient values was up to ± 100%. For converging flow methods using the Cogswell model the variation in extensional viscosity values was estimated to be up to ± 230%. In comparing peak transient extensional viscosity values obtained from stretching methods with "equilibrium" values obtained by the other methods, the level of agreement was considered to be good with significant overlap of data from the different methods being obtained. This finding supports the use of converging flow methods for determining extensional viscosity values, albeit "equilibrium" values.

ISSN 1361-4061

National Physical Laboratory
Teddington, Middlesex, UK, TW11 0LW

Prepared as a deliverable of milestone 6 of the project
MMP11: Measurement of extensional viscoelastic properties of polymers,
a project of the Department of Trade and Industry EID programme
on measurements related to the processability of materials

Approved on behalf of Managing Director, NPL
by Dr C Lea, Director, Centre of Materials Measurement and Technology

CONTENTS

1. INTRODUCTION

Although extensional flow properties of polymer melts play an important role in their behaviour in processing, these properties are rarely characterised compared with that of their shear flow properties. This is partly due to the longer history and greater use of flow simulation software for injection moulding, for example Moldflow, that requires shear flow properties. In injection moulding simulation it is assumed that the contribution due to the extensional flow behaviour is negligible. This assumption may be reasonable but in places such as on entering the gate or in radial flow, the extensional flow behaviour will contribute to the filling behaviour. In other processes, for example blow moulding, film blowing and, to a lesser degree, in extrusion the extensional properties will be predominant in influencing the material's flow behaviour.

Extensional flow properties of materials were, according to Ballman [1], first studied by Trouton [2] in 1906 on pitch, tar and wax materials. It was observed that the extensional viscosity values were approximately three times the shear viscosity values, yielding what is now commonly referred to as the Trouton ratio. Research into the measurement of extensional flow properties progressed in the 1960s with work on PS reported by Ballman [1] in 1965. Significant advances of the study of the extensional properties of polymer melts were then made by Cogswell [3] in 1968 and Meissner [4] in 1969 with the development of new instruments. A period of activity followed in the 1970s (predominantly but not exclusively by Meissner, Münstedt and Laun) that was based largely on the instruments of Cogswell [3] and Meissner [4] or developments thereof. Since the early work of Cogswell [3] and Meissner [4] several articles and reviews describing the various extensional viscoelastic methods for polymer melts have been written in both journals and texts [5-14]. The reviews of Meissner [5, 6] focused in particular on the techniques developed by Meissner [15] and Münstedt [16].

Intercomparisons of the extensional flow behaviour of polymer solutions have indicated very significant variations in the measured behaviour. Measurements of the shear and extensional viscoelastic properties of three polymer solutions M1, A1 and S1 have been reported by various researchers:

> M1 - 0.244% polyisobutylene in a mixed solvent of 7% kerosene in polybutene, exhibiting constant shear viscosity with a dominant relaxation time of 0.3 s [references 17 (26 papers) and 18];
>
> A1 - 2% polyisobutylene in a mixture of cis- and trans-decalin, exhibiting shear thinning with a dominant relaxation time of 5 s [references 18 and 19]; and
>
> S1 - 2.5% polyisobutylene in a mixture of decalin and polybutene, exhibiting shear thinning with a dominant relaxation time similar to M1 [reference 20 (7 papers)].

The experimental methods that were used are described in the various papers and also by James et al [21] and Gupta et al [8]. Comparison of results for the polymer solutions A1 [19] and M1 [21] clearly indicated substantial differences in extensional properties obtained using the different methods: the extensional viscosity varied by three decades over the two decades of strain rate with results presented over virtually the entire region. Petrie [22] commented that the discrepancy was because "the experimental methods were not reproducing the conditions equivalent to the formal definition of extensional viscosity" - i.e. the tests generated flow fields that were not well approximated by the mathematical descriptions used to interpret the experimental data. James et al [21] commented that the rheometers used in the study of the fluid M1 should be viewed as yielding *"an* extensional viscosity rather than *the* extensional viscosity".

In terms of comparing measurements for polymer melts, Münstedt et al [23] made steady state measurements of extensional viscosity of LDPE and HDPE using different instruments. One instrument had rotating clamps and the other translating clamps. He observed that there was good agreement of results between the two methods, although these two instruments are significantly more similar than the broad range of instruments used in the intercomparison studies of polymer solutions described earlier.

Extensional techniques can be described, following Nazem et al [24], as "controllable" or "non-controllable" [12, 13]. "Controllable" implies that the instantaneous values of strain rate and stress are uniform throughout the specimen and that the strain rate or stress is held constant with time. The results of non-controllable methods (e.g. constant force or variable strain rate) for example fibre spinning and converging flow analysis [7, 8, 25] tend to be difficult to interpret [10]. This is emphasised by Gupta et al [8] who commented that uniaxial stretching methods are the preferred methods for obtaining fundamental data but can only be performed on very viscous polymers and at low strain rates. Cogswell [11] also concluded that constant speed or constant force methods provide no information that cannot be provided better by the "direct measurement" constant stress or constant strain rate methods.

The work on polymer solutions has clearly highlighted some of the difficulties facing the measurement of extensional flow properties. The purpose of this intercomparison is to assess the level of agreement between extensional flow methods for characterising polymer melts, including the use of “controllable” and “non-controllable” methods.

2. INTERCOMPARISON BASIS

The intercomparison was based principally on the use of tensile stretching and converging flow methods. The latter method is based on the interpretation of entrance pressure drop data, obtained from the converging flow region upstream of the die in capillary extrusion rheometry, as extensional viscosity data. The entrance pressure drop data can be interpreted using, for example, the Cogswell model [26]. Also, fibre spinning and a further method based on flow visualisation in a converging flow, using stress birefringence and velocity measurements of seed particles to determine the stress and velocity fields, were included in the intercomparison.

The intercomparison was carried out on the basis that the participating laboratories were each supplied a sample of a high density polyethylene taken from the same batch. Testing was carried out at 150 ºC and 190 ºC. Two temperatures were chosen as it was likely that not all the methods would be able to characterise the material at a single temperature. Thus a greater range of methods have been incorporated in the intercomparison than had a single temperature been used.

No constraints were placed on the methods to be used except that strain rates of 0.01, 0.1, 1, 3 and 10 s^{-1} were recommended for testing, where possible, to aid comparison of results. Specimen preparation was carried out, where necessary, by the participating laboratories due to the different requirements of the instruments involved in the intercomparison. Thus results of the intercomparison may also reflect differences due to different specimen preparation procedures. All the results were collated and compared by the NPL.

3. MATERIAL

A high density polyethylene (HDPE) was chosen for use in this intercomparison. Oscillatory rheometry testing indicated that the HDPE (NPL reference HGH000) was very stable over approximately 2 hour at 190 ºC with shear moduli values G’ and G’’ changing by less than 5% over that period, Figure 1. A temperature scan, also carried out using an oscillatory rheometer, indicated a melt transition temperature of approximately 120 ºC and a temperature dependence of shear moduli of the order of 0.5%/ºC, Figure 2. At the temperatures of 150 ºC and 190 ºC that were selected for testing no sharp transitions in behaviour were observed. Thus the effect of differences in average test temperature between laboratories would be minimal. However, spatial temperature variations in tensile testing may have a significant effect on results [27]. Furthermore, initial testing indicated that the material exhibited an intermediate level of strain hardening [28]. It was considered undesirable to select a material for the intercomparison that exhibited either very little strain hardening or a high degree of strain hardening.

4. DESCRIPTION OF TEST METHODS

4.1 TENSILE STRETCHING FLOW METHODS

A range of tensile stretching methods were used in the intercomparison. In summary, they included stretching between translating clamps, i.e. the standard tensile testing configuration in which the clamps move relative to one another along the same axis (L3, L16)[1], between a fixed and a rotating clamp (L8, L9, L10) and between rotating clamps (L6).

Other significant differences between the methods were in the preparation of the specimens and in the geometry and aspect ratio of the specimens. L3 and L6 prepared specimens by compression moulding, L16 by transfer moulding and L8, L9 and L10 by extrusion. L3 and L6 used specimens of rectangular cross-section whilst L8, L9, L10 and L16 used specimens of circular cross-section. For the circular cross-sectioned specimens the aspect ratios (length/diameter) were greater than 10:1 except for L16 in which case it was ≈ 4:1. For the rectangular cross-sectioned specimens, the aspect ratio (length/width) was ≈ 2.3:1 for L3, and 8:1 for L6 (the width is taken to be the larger of the two remaining non-length dimensions).

4.2 CONVERGING FLOW METHODS

All the participating laboratories used the Cogswell converging flow model [26] for interpreting the entrance pressure drop data in terms of extensional viscosity. All laboratories used a flat entry geometry. However, the method for determining the entrance pressure drop data varied from laboratory to laboratory.

Short dies (≈ 0.25 mm in length) were used by L12 and L17 and the extrusion pressures obtained for those dies were taken as the entrance pressure drop values (i.e. the data were not extrapolated to a true zero length). Analysis of the determination of entrance pressure drop values for L12 indicated that this may result in values ≈ 10% greater than had extrapolation to zero length been carried out.

Extrapolation of data obtained using at least two dies to a die length of zero, following the principle proposed by Bagley [29], was carried out by L5, L7, L9 and L14. In addition, one laboratory (L7) determined the entrance pressure drop values by two methods: by using a linear fit and also a polynomial fit to the extrusion pressure - die length/radius ratio data. The difference in determined values as a consequence of the different methods adopted by L7 is considered below.

In addition to these measurements, L19 used an oscillatory rheometer to characterise the dynamic behaviour of the HDPE, the results of which have been compared with capillary rheometry data by using the Cox-Merz relationship to equate dynamic with steady shear data [30].

4.3 FIBRE SPINNING AND FLOW VISUALISATION METHODS

Other methods employed in the intercomparison were fibre spinning and flow visualisation techniques.

Fibre spinning techniques were used by two laboratories L1 and L4, both at 190 °C only. The procedures used by the two laboratories were significantly different. L1 used a constant extruder throughput combined with different constant accelerations of the winding wheel to produce different test profiles of increasing strain and strain rate. In comparison, L4 used different extruder throughput rates combined with the same winding wheel speed profile to produce different test profiles of increasing strain and strain rate. The analysis used by L1 to interpret data was also applied to the data obtained by L4 to enable a more appropriate comparison of the results to be made.

[1] L is used herein to indicate laboratory, thus L3 corresponds to laboratory no. 3.

The flow visualisation method (L18) used laser velocimetry particle tracking to determine the velocity field, and hence the local strain rates, and stress birefringence to determine the stress field. From these data extensional viscosities for the planar flow were derived. The contraction ratio for the planar flow was 5:1. Obviously, agreement of data obtained with this technique with the other methods is not expected as it generates a planar extensional flow field and thus planar extensional viscosities. Nevertheless, comparison of the data with uniaxial extensional data is of interest. Petrie [7] indicated that the planar extensional viscosity for a Newtonian fluid, and also for various other constitutive forms, is equivalent to four times the shear viscosity, compared with a ratio of three for uniaxial extensional viscosity. One might therefore expect higher planar than uniaxial extensional viscosity values, although there is no reason to assume that the behaviour of the HDPE fits one of the constitutive forms for which these ratios are valid.

5. RESULTS

5.1 TENSILE STRETCHING FLOW RESULTS

Comparison of data obtained by stretching methods at 150 ºC indicates a broad agreement of results, Figure 3. Data are plotted as extensional stress growth coefficient values[2] as a function of time. Data obtained at all strain rates are plotted as such data form an apparent master curve. The data depart from this master curve at high strains due to additional "strain hardening". The point of departure from the master curve is dependent on the strain rate: the lower the strain rate the further along the master curve the departure occurs. The data supplied by participating laboratories have been trimmed to remove spurious data obtained at very short times and also at the end of the test where the data indicated that the specimen had failed, observed as a sudden down-turn in the curve. Data were obtained at strain rates in the range approximately 0.01 - 10 s^{-1}.

The variation in data was greatest at short times, Figure 3. Removal of L3 data and L8 short-time data reduced this variation considerably, Figure 4. For clarity, data obtained by the laboratories are presented individually in Figures 5 - 10. The repeatability of measurements was good being generally within $\pm$ 10% at all but short times/low strains, Figures 5, 7, 8, 10. It was observed that L16 data exhibited no additional strain hardening, Figure 10. This was probably due to the voidage in the specimens (produced by transfer moulding) as reported by L16. It is suggested that the voids prevented additional strain hardening from occurring by causing each specimen to fail prematurely at a void.

Results obtained at $\approx$1 s^{-1} only and at 150 ºC, Figure 11, show a similar level of scatter to the data obtained at all strain rates, Figure 3. Thus this indicates that plotting all strain rate data together is an acceptable procedure. The variation in extensional viscosity data at 150 ºC (excluding that due to additional strain hardening that is considered separately later) was estimated to be up to $\pm$ 60% at short times (0.1 s) and $\pm$ 30% at long times (70 s), Figure 4.

To assess the effect of strain rate on the data, the maximum transient stress growth values, i.e. the values at failure (except in the case of L3 for which the maximum strain of $\approx$ 3.3 was achieved without failure[3]) are presented as a function of strain rate, Figure 12. A power-law was fitted to the data. The one standard deviation value from the best-fit line was of the order of $\approx$ 50%. L16 results are lower than the mean, presumably due to the lack of strain hardening measured by that laboratory, while L3 data are higher. Exclusion of L3 and L16 data would result in a higher negative gradient of the line with a good fit to the data obtained by the remaining laboratories L6, L8, L9 and L10.

Results are similarly presented for testing at 190 ºC, Figure 13. However, fewer laboratories returned results at 190 ºC, in part as they were unable to test at the higher temperature. Again the removal of L3 results

[2] See Appendix for definition of terms.
[3] The experimental set up resulted in a limit of $\approx$ 3.3 for the maximum achievable Hencky strain.

reduced the scatter in measured values, Figure 14, although L3 data were similar to the data obtained by other laboratories at higher strains, as was also the case at 150 ºC. The variation in extensional viscosity data at 190 ºC (excluding that due to additional strain hardening that is considered later) was typically up to ± 35%, although very low (0.01 s^{-1}) and high rate (6.28 s^{-1}) L9 data fell outside this range, Figure 14. Again, results obtained by individual laboratories are plotted separately, Figures 15 - 18.

The maximum transient stress growth values, i.e. at failure in all test cases including L3, are presented as a function of the strain rate, Figure 19. Analysis yielded a standard deviation value of the data from the best-fit line to be of the order of ≈ 40% which is similar to that obtained at 150 ºC.

It is suggested that the difference between the stretching flow results obtained by L3 and those obtained by other laboratories may have been due to the low aspect ratio (2.3:1) of the specimens used by L3, resulting in significant end-errors. Vinogradov et al [31] indicated that an aspect ratios of at least x10 should preferably be used.

5.2 CONVERGING FLOW RESULTS

Shear viscosity data are also required to interpret entrance pressure drop data in terms of extensional viscosity values using the Cogswell converging flow model [26]. Thus results of shear viscosity measurements at 150 ºC and 190 ºC are also presented, Figures 20 and 23 respectively. Lab 19 results are based on the use of an oscillatory rheometer. On applying the Cox-Merz rule [30] L19 data are in good agreement with capillary rheometry data. The variation in shear viscosity data is estimated to be up to ± 60% at 150 ºC and up to ± 25% at 190 ºC.

Entrance pressure drop data at 150 ºC and 190 ºC are presented in Figures 21 and 24 respectively. The variation in the data is up to approximately ± 160% at 150 ºC and up to approximately ± 180% at 190 ºC, excluding the data derived by L7 using a quadratic rather than linear fit for analysis of the Bagley plots (data references “L7 … Quad”).

The effect of using either a linear or quadratic fit to the Bagley plots by L7 was significant. Entrance pressure drop data fitted using a quadratic were on average 25% higher than the equivalent values determined using a linear fit to the same extrusion pressure data, Figure 24. Its effect on shear viscosity values was less significant but was still averaging in the order of 4 - 18% lower when using the quadratic fit, depending on the die length values used by L7 to calculate the shear viscosity values. Of significance is the fact that a higher entrance pressure drop and a lower shear viscosity, as is the consequence of using a quadratic fit, both have the same effect of increasing the predicted extensional viscosity, by ≈ 50% in this case as is observed in Figure 25.

Extensional viscosity values derived from the shear viscosity and entrance pressure drop data using the Cogswell model [26] are presented in Figures 22 and 25. The range in extensional viscosity values was up to approximately ± 220% at 150 ºC and approximately ± 230% at 190 ºC, again excluding the L7 quadratic fit data (data references “L7 .. Quad”). It is noted that there was no observed correlation between the magnitude of the extensional viscosity values obtained by the various laboratories and the contraction ratios used (i.e. ratio of barrel cross-sectional area to die cross-sectional area).

The most extensive repeat testing carried out was by L17 at 150 ºC and indicated a variation in data of up to ± 8% in shear viscosity, ± 20% in entrance pressure drop and ± 50% in extensional viscosity, Figures 20 - 22 respectively.

5.3 FIBRE SPINNING AND FLOW VISUALISATION RESULTS

Fibre spinning measurements were carried out by two laboratories, L1 and L4. L1 carried out measurements using the same die extrusion rate but different wheel accelerations (and thus haul-off speeds), whereas L4 carried out measurements using the same wheel haul-off speeds but different die extrusion rates. Extensional viscosity values plotted as functions of strain rate and strain indicate a total variation in extensional viscosity values of approximately x10, Figures 26 and 27 respectively. Within each laboratory, a variation in extensional viscosity values with different testing conditions of approximately x3 was obtained.

It is noted that the thus determined extensional viscosities were relatively independent of strain rate or strain, Figures 26 and 27. However, in these tests an increase in strain rate also corresponded to an increase in strain. An increase in strain rate would result in a reduction in extensional viscosity for a given strain, whilst an increase in strain would result in an increase in extensional viscosity for a given strain rate. Thus the two factors, having opposite effects on extensional viscosity, would tend to cancel each other thus resulting in a greater apparent independence of extensional viscosity on either parameter. The cause or causes of the difference in results between these two laboratories, averaging in the order of x4, are not clear from these results, except to say that the differences between the procedures used, for what is fundamentally the same technique, were significant.

The results obtained using the flow visualisation method, L18 at 190 ^{o}C, have been compared with the data obtained from the converging flow methods, Figure 25 (also compare L18 data with Figure 29). The flow visualisation results are lower than the converging flow results at corresponding strain rates. However, the strain rate dependence of extensional viscosity (i.e. the gradient of the plot) is similar, except at the highest strain rates at which point extensional viscosity values start to increase. Thus the original expectation that the planar viscosities should be higher than the uniaxial extensional viscosities (Section 4.3) has not been realised. To possibly account for this, it is noted that the flow visualisation method is non-controlled. The determination of extensional viscosity data is complicated in that the low strain rate data corresponds to low strains and the high strain rate data to higher strains. Furthermore, it is noted that the maximum Hencky strain for the flow visualisation measurements is small at approximately 1.6 (area contraction ratio of 5:1) whereas for the converging flow measurements it is higher, being in the range 3.1 - 5.5 (area contraction ratios of 22.6:1 - 225:1). It is expected that these factors would contribute to any discrepancy between the methods.

6. COMPARISON OF RESULTS FROM ALL METHODS

The results of all uniaxial extensional viscosity measurements are compared in Figures 28 and 29. The maximum extensional stress growth coefficient values obtained from stretching methods (presented separately as Figures 12 and 19) are plotted for comparison with the converging flow and fibre spinning methods (the later at 190 °C only). There is good overlap of data obtained by the stretching and converging flow methods over at least one decade of strain rates at 150 °C, Figure 28.

Similarly, the overall level of agreement is considered to be good for data at 190 °C, with data obtained using the three approaches occupying broadly the same region of the plot, i.e. $\approx 10^6$ Pa.s at ≈ 1 s^{-1} (excluding L4 fibre spinning data), Figure 29.

At both temperatures, but especially at 150 °C, the stretching and converging flow data have similar strain rate dependencies, given by the gradient of the data. However, this is not the case for the fibre spinning data for the reasons discussed in Section 5.3.

7. DISCUSSION

As discussed in the introduction, different methods may be either controlled or non-controlled. The tensile stretching flow results (Section 5.1) were obtained under controlled conditions, i.e. constant strain rate, whereas those obtained by converging flow methods (Section 5.2) and flow visualisation and fibre spinning methods (Section 5.3) were under non-controlled conditions.

The converging flow methods are considered to be non-controlled as data are obtained from tests in which the strain rate varies through the converging region, but the total strain of deformation is fixed by the ratio of the barrel diameter to die diameter of the capillary extrusion rheometer. The data thus obtained are nominally "equilibrium" extensional viscosity data as the Cogswell model used in the interpretation of the experimental data assumes equilibrium extensional viscosity behaviour. Similarly, fibre spinning is a non-controlled method as the strain rate varies along the fibre length.

Thus comparison of data obtained by the various methods is complicated by the differences in the strain rate histories that the material undergoes in each of the various test methods. Despite these fundamental differences in the methods, reasonable agreement of data from the stretching flow and converging flow methods was obtained, and to a lesser degree there was agreement with some of the data obtained from fibre spinning measurements.

8. CONCLUSIONS

An intercomparison of extensional flow characterization techniques for polymer melts has been presented. The methods used in the intercomparison were tensile stretching, converging flow, fibre spinning and flow visualisation. A high density polyethylene that was stable at 190 °C for in excess of two hours was used as the intercomparison material. The results demonstrate the level of agreement obtained within each measurement method type, and also the level of agreement between the different measurement method types.

- For tensile stretching methods the variation in extensional stress growth coefficient values was estimated to be up to ± 60%, although the variation in peak extensional stress growth coefficient values as a function of strain rate was greater at up to approximately ± 100%.

- For converging flow methods the variation in extensional viscosity values was estimated to be up to ± 230%. This comprised of variations in the determination of shear viscosity estimated to be up to ± 60% at 150 °C or ± 25% at 190 °C, and also in entrance pressure drop estimated to be up to ± 160% at 150 °C or ± 180% at 190 °C.

- In comparing peak transient extensional viscosity values obtained from stretching methods with "equilibrium" values obtained by the other methods, the level of agreement was considered to be good with significant overlap of data from the different methods being obtained. This finding supports the use of converging flow methods for determining extensional viscosity values, albeit "equilibrium" values.

9. ACKNOWLEDGEMENT

The work reported in this paper was carried out as part of a project on measurement of the extensional viscoelastic properties of polymers (MMP11, milestone 6). This project is part of a programme of underpinning research financed by the Engineering Industries Directorate (EID) of the Department of Trade and Industry on measurements related to the processability of materials.

The authors would also like to thank the material supplier and also the participating organisations in the intercomparison:

Alpha Technologies UK, UK; BP Chemicals snc, France; BP Chemicals, Grangemouth, UK; CRNC-NRC, Canada; DSM Research, Netherlands; ETH, Switzerland; Huels AG, Germany; Institute of Polymer Technology and Materials Engineering, Loughborough University, UK; IRC Polymer Science and Technology, University of Bradford, UK; Laboratoire De Rheologie Des Matieres Plastiques, France; PCD Polymere, Austria; University of Minho, Portugal; Yamagata University, Japan.

10. REFERENCES

1 R.L. Ballman, Rheol. Acta, 4 (1965) pp.137-140.
2 F.T. Trouton, Proc. Roy. Soc., A77 (1906) pp.426.
3 F.N. Cogswell, Plastics and Polymers, April 1968, pp.109-111
4 J. Meissner, Rheol. Acta, 8 (1969) pp.78-88.
5 J. Meissner, Chem Eng. Commun., 33 (1985) pp.159-180.
6 J. Meissner, Polym. Eng. Sci., 27 No. 8 (1987) pp.537-546.
7 Elongational Flows, C.J.S. Petrie, Pitman, London, 1979.
8 R.K. Gupta and T. Shridar, Elongational Rheometers, in Rheological Measurement, Ed. A.A. Collyer and D.W. Collyer, Elsevier Applied Science, London, 1988.
9 J.M. Dealy, Polym. Eng. Sci., 11 (1971) pp.433-445.
10 J.M. Dealy, J. Non-Newtonian Fluid Mech., 4 (1978) pp.9-21.
11 F.N. Cogswell, Trans. Soc. Rheol., 16 (1972) pp.383-403.
12 Rheological Techniques, R.W. Whorlow, Ellis Horwood, London, 1992.
13 Rheometry, K. Walters, Chapman and Hall, London, 1975.
14 Rheometers for Molten Plastics, J.M. Dealy, Van Nostrand Reinhold Company, London, 1982.
15 J.M. Meissner, Trans. Soc. Rheol., 16 (1972) pp.405-420.
16 H. Mnstedt, J. Rheology, 23 (1979) pp.421-436.
17 Proceedings of an International Conference on Extensional Flow, Combloux, France, March 20-23 1989. Special Issue of J. Non-Newtonian Fluid Mechanics, July 1990.
18 V. Tirtaatmadja and T. Sridhar, J. Rheology, 37 (1993) pp.1081-1102.
19 N.E. Hudson and T.E.R. Jones, J. Non-Newtonian Fluid Mechanics, 46 (1993) pp.69-88.
20 Proceedings of a meeting on The Rheometry of Polymer, from the solution to the melt, Abbaye Royale de Fontevraud, May 12-15 1993. Special Issue of J. Non-Newtonian Fluid Mechanics, May 1994.
21 D.F. James and K. Walters, A Critical Appraisal of Available Methods for the Measurement of Extensional Properties of Mobile Systems, in Techniques in Rheological Measurements, Ed. A.A. Collyer, Chapman and Hall, London, 1993.
23 H. Münstedt and H.M. Laun, Rheol. Acta, 20 (1981) pp.211-221.
22 C.S. Petrie, Rheol. Acta, 34 (1995) pp.12-26.
24 F. Nazem and C.T. Hill, Trans. Soc. Rheol., 15 (1974) pp.87.
25 D.M. Binding, Contraction Flows and New Theories for Estimating Extensional Viscosity, in Techniques in Rheological Measurements, Ed. A.A. Collyer, Chapman and Hall, London, 1993.
26 F.N. Cogswell, Polym. Eng. And Sci., 12 No.1, Jan. 1972, pp.64-73.
27 J. Meissner, T. Raible and S.E. Stephenson, J. Rheology, 25 (1981) pp.1-28.
28 Rides, M, Extensional flow properties of polymer melts: Their measurement and effect on processing performance, NPL Report CMMT(B)200, August 1998, National Physical Laboratory, UK.
29 E.B. Bagley, J. Applied Physics, 28 No.5 (1957) pp.624-627.
30 W.P. Cox and E.H. Merz, J. Polym. Sci., 28 (1958) pp.619-622.
31 G.V. Vinogradov, V.D. Fikhman, B.V. Radushkevich and A.Ya. Malkin, J. Polym. Sci., A-2, 8 (1970) pp.657-678.
32 J.M. Dealy, J. Rheology 39(1) January/February 1995, pp.253-265.

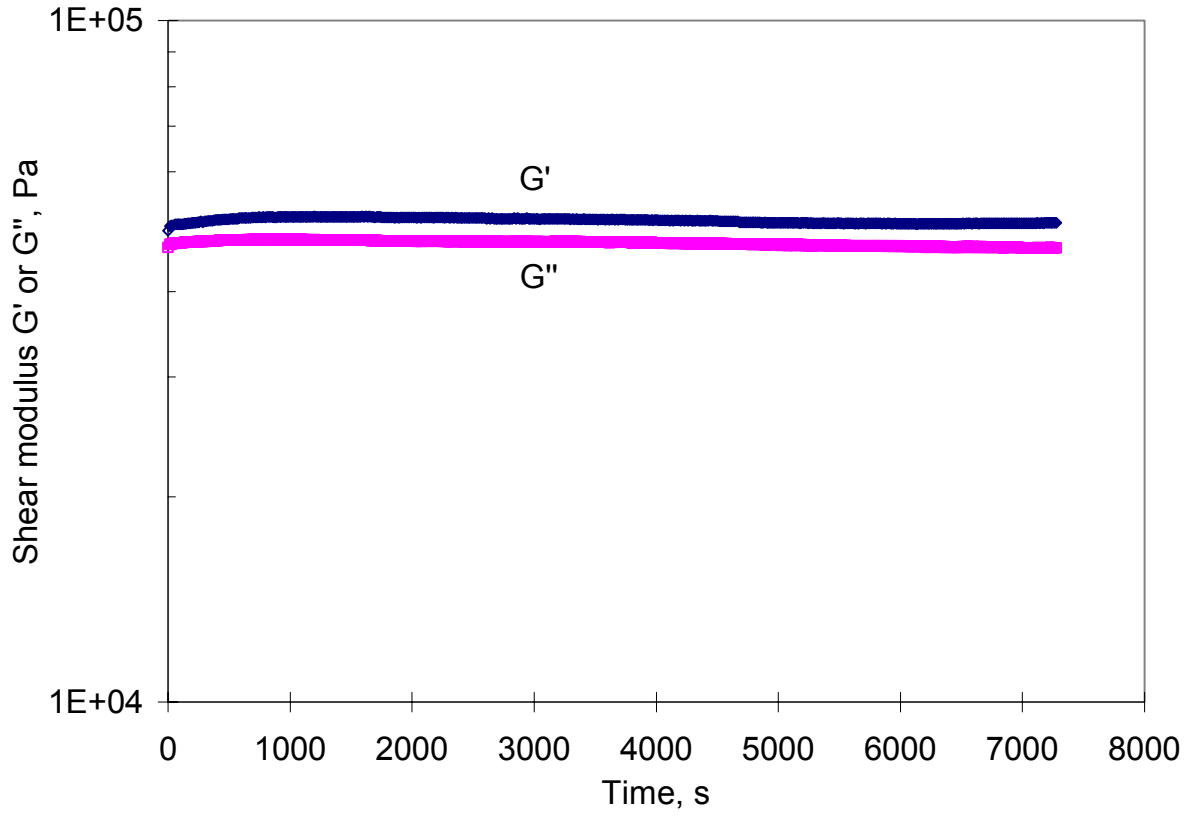

Figure 1 Evaluation of the thermal stability of a HDPE (HGH000) at 190 ºC using an oscillatory rheometer.

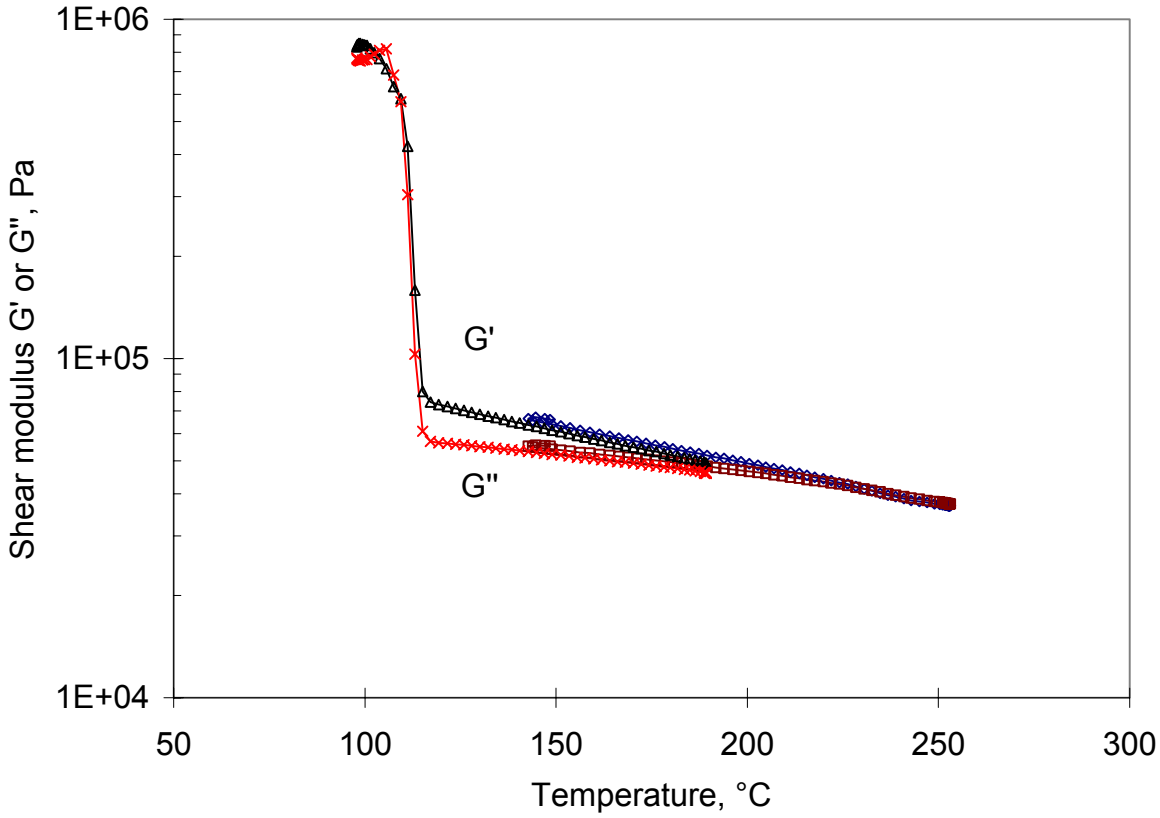

Figure 2 Evaluation of the temperature dependence of a HDPE (HGH000) using an oscillatory rheometer.

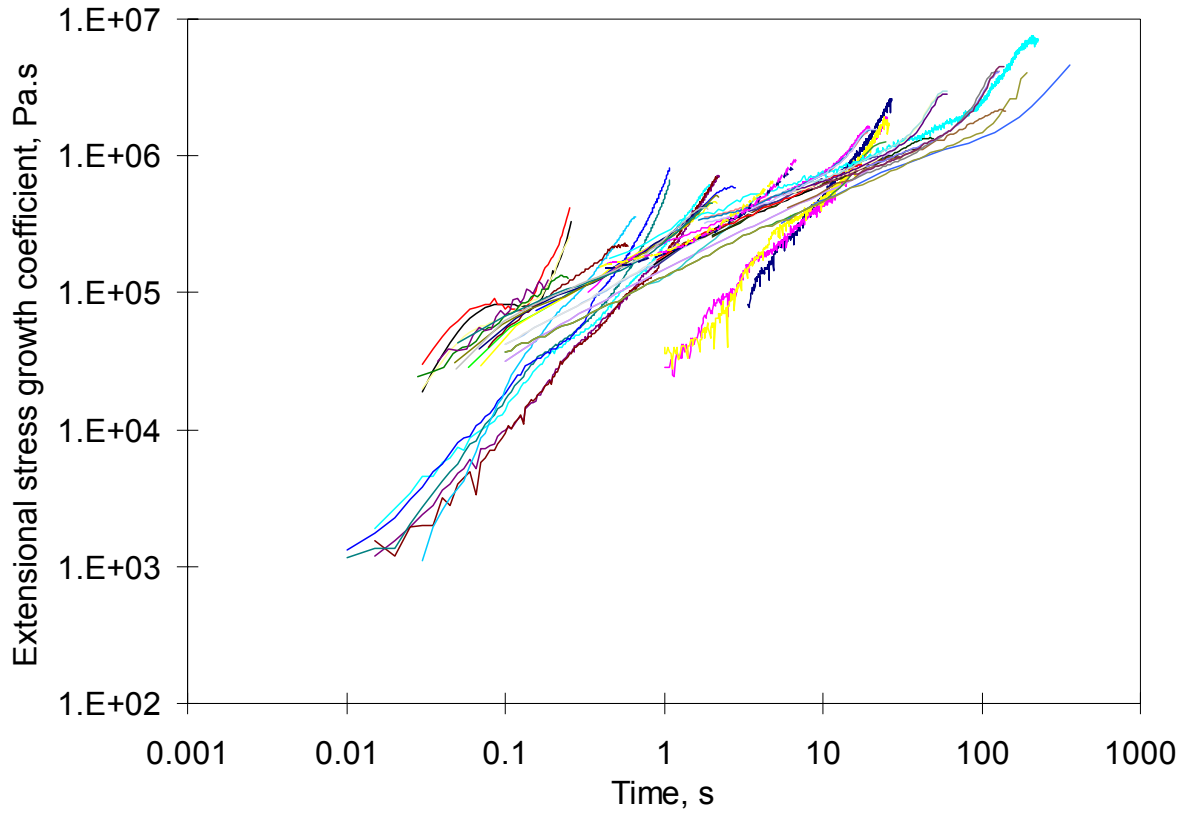

Figure 3 Intercomparison of stretching flow methods for a HDPE (HGH) at 150 ºC: all data.

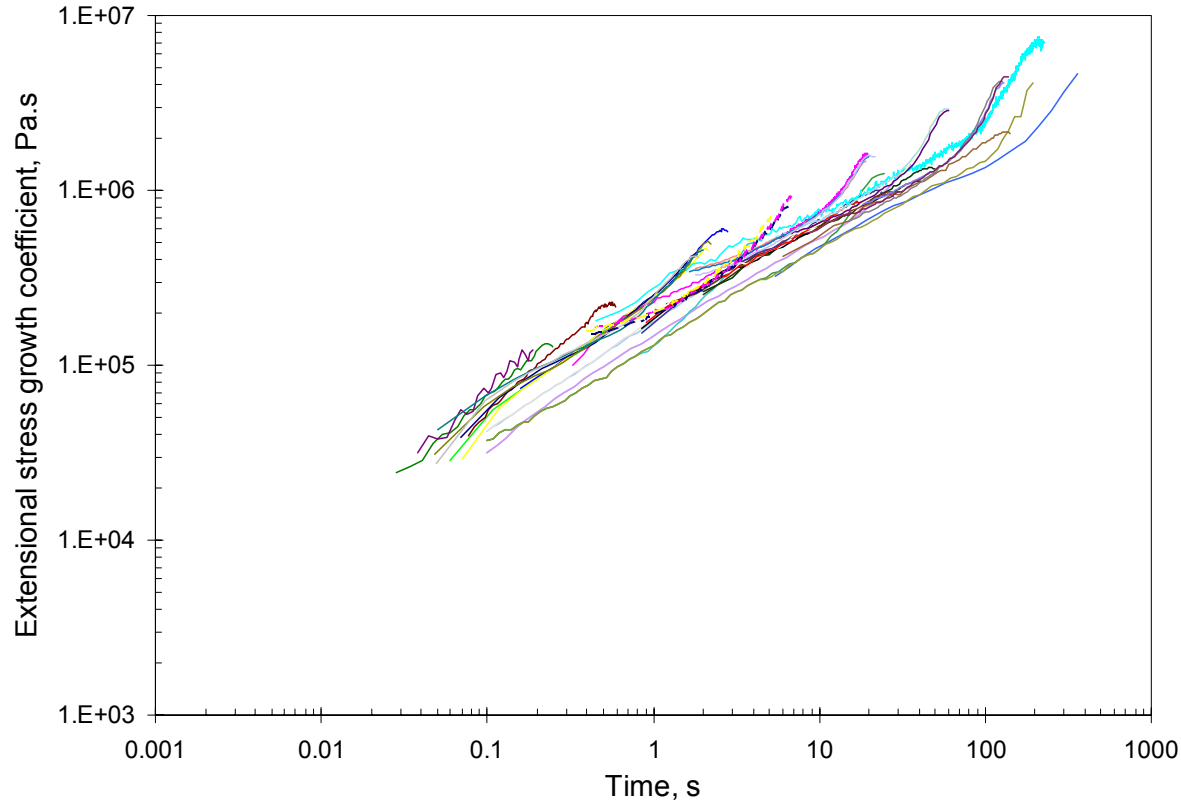

Figure 4 Intercomparison of stretching flow methods for a HDPE (HGH) at 150 ºC: laboratory 3 and short time laboratory 8 data removed.

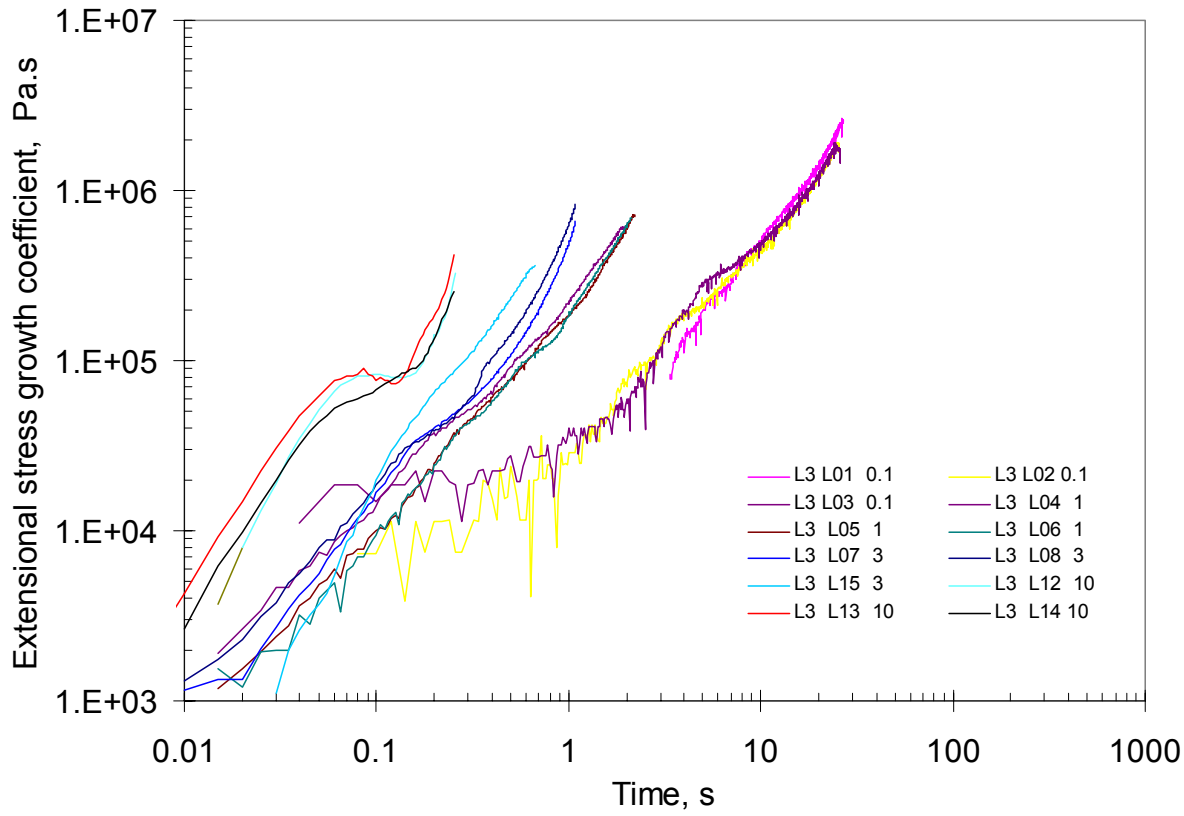

Figure 5 Extensional stress growth coefficient data for laboratory 3 for a HDPE (HGH) at 150 ºC.

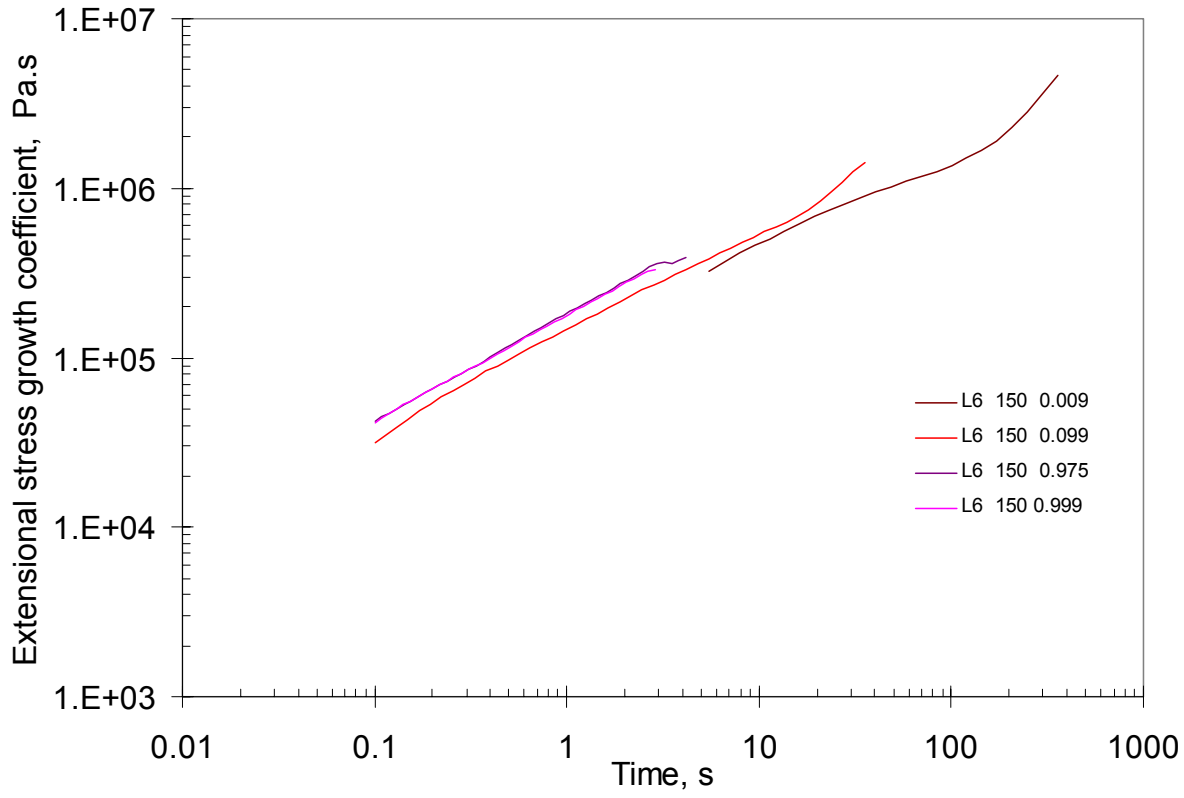

Figure 6 Extensional stress growth coefficient data for laboratory 6 for a HDPE (HGH) at 150 ºC.

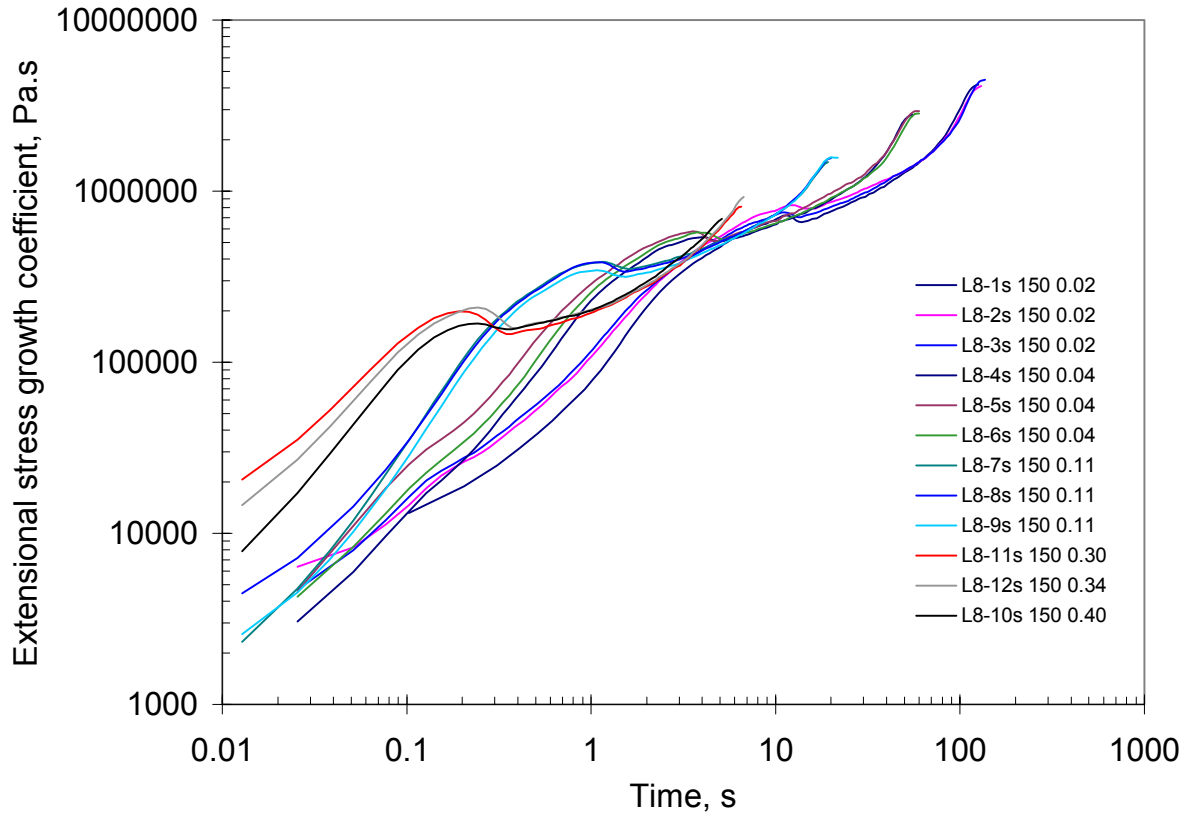

Figure 7 Extensional stress growth coefficient data for laboratory 8 for a HDPE (HGH) at 150 ºC.

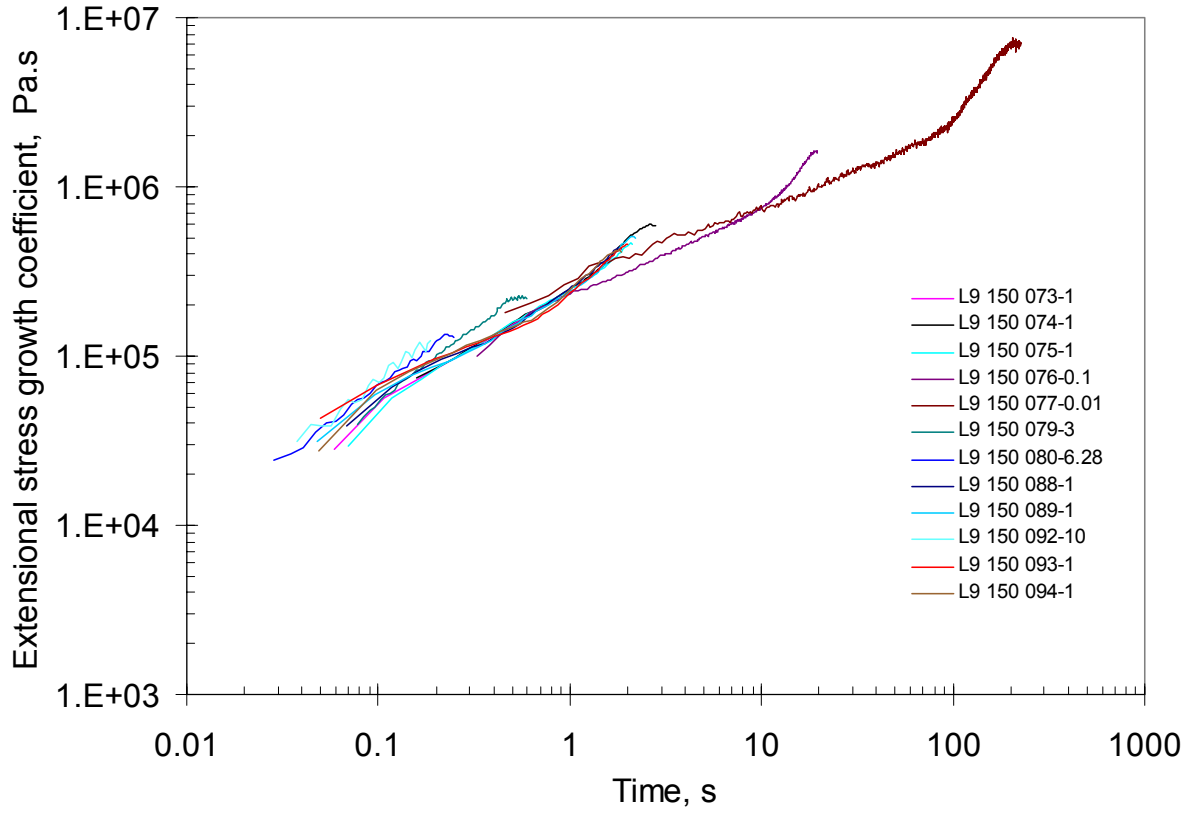

Figure 8 Extensional stress growth coefficient data for laboratory 9 for a HDPE (HGH) at 150 ºC.

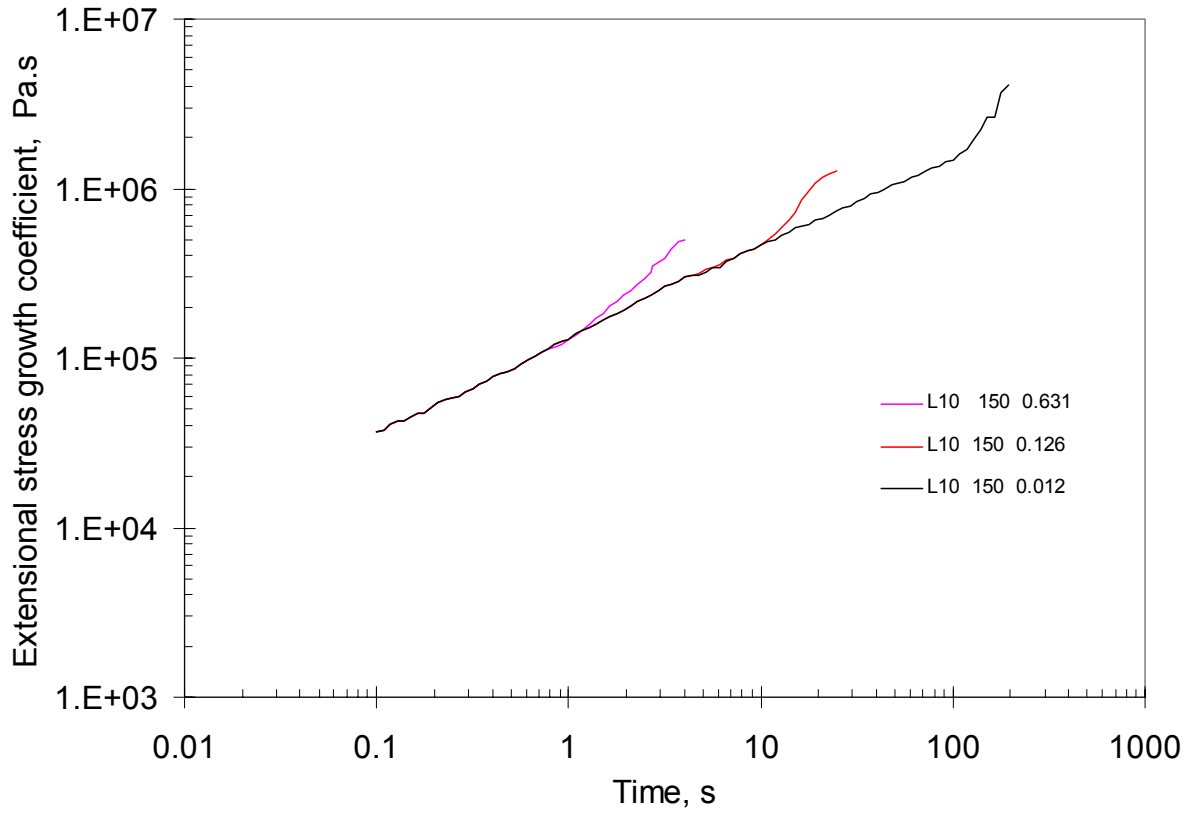

Figure 9 Extensional stress growth coefficient data for laboratory 10 for a HDPE (HGH) at 150 ºC.

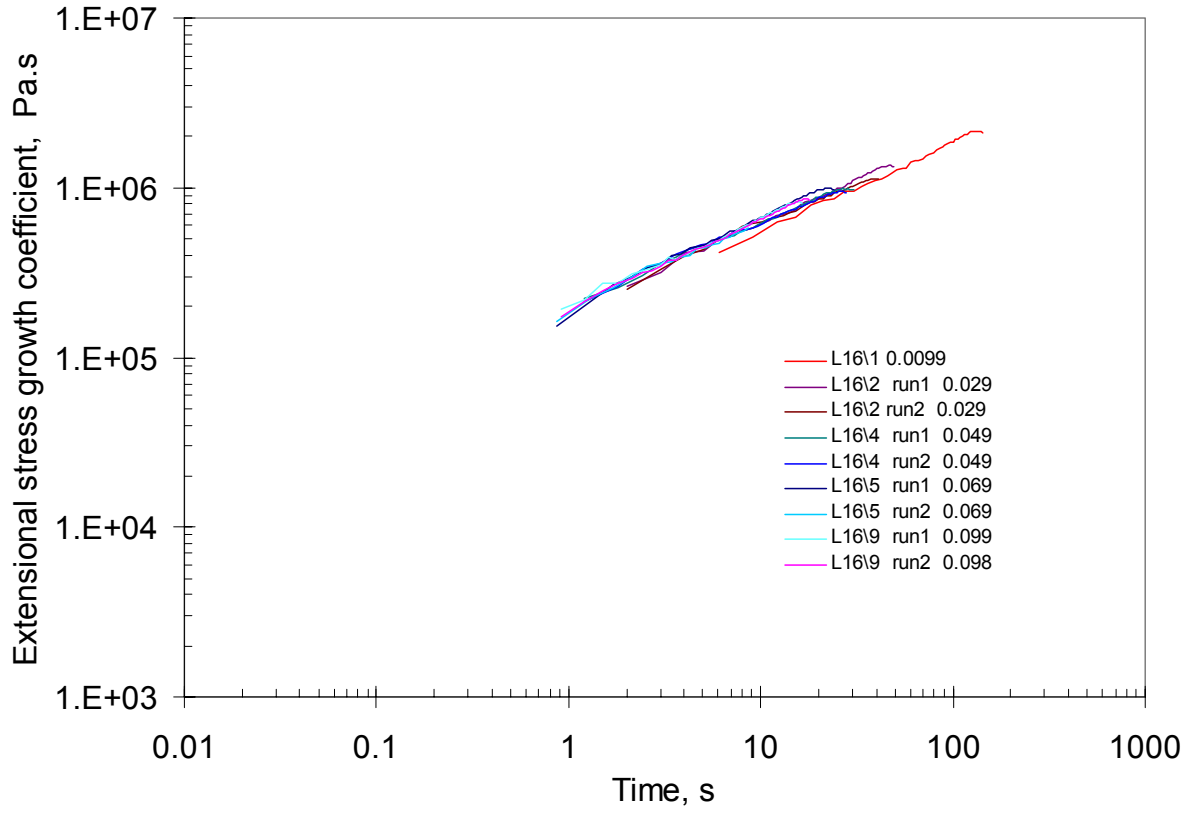

Figure 10 Extensional stress growth coefficient data for laboratory 16 for a HDPE (HGH) at 150 ºC.

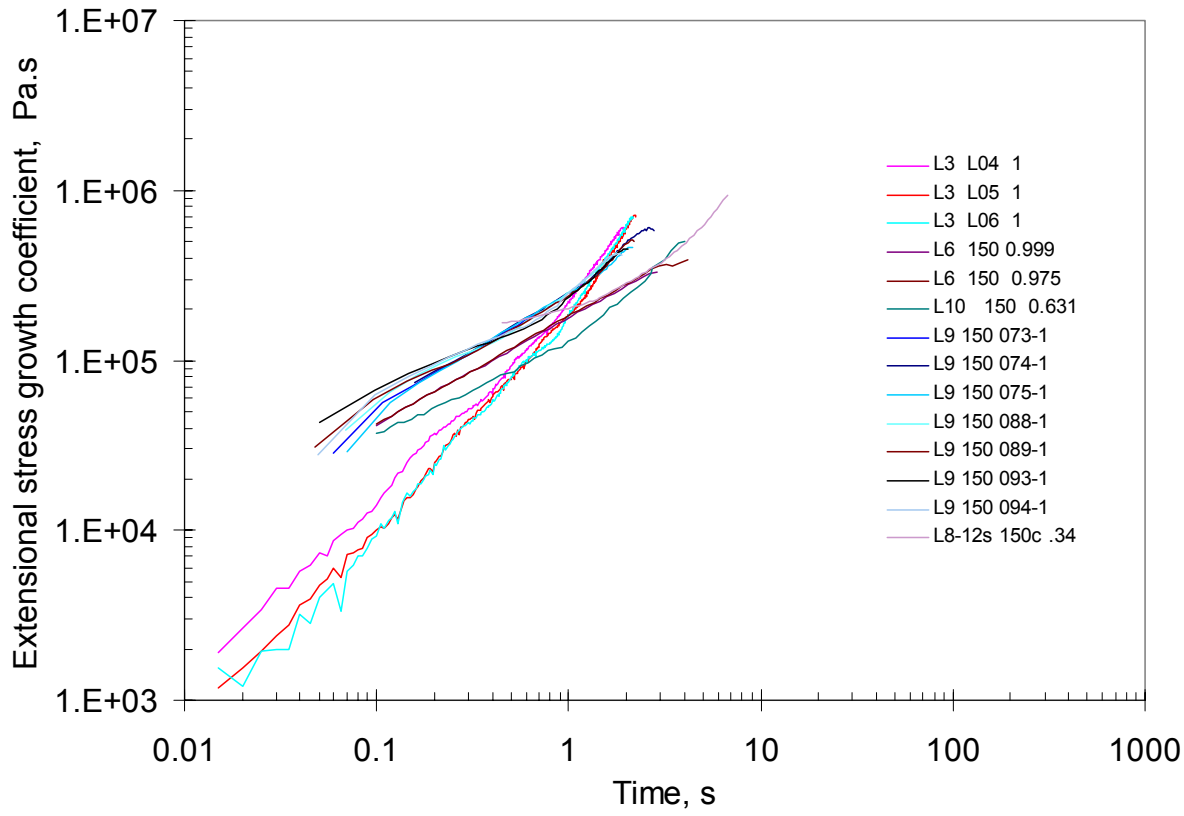

Figure 11 Intercomparison of stretching flow methods for a HDPE (HGH) at approximately 1 s^{-1} and 150 ºC.

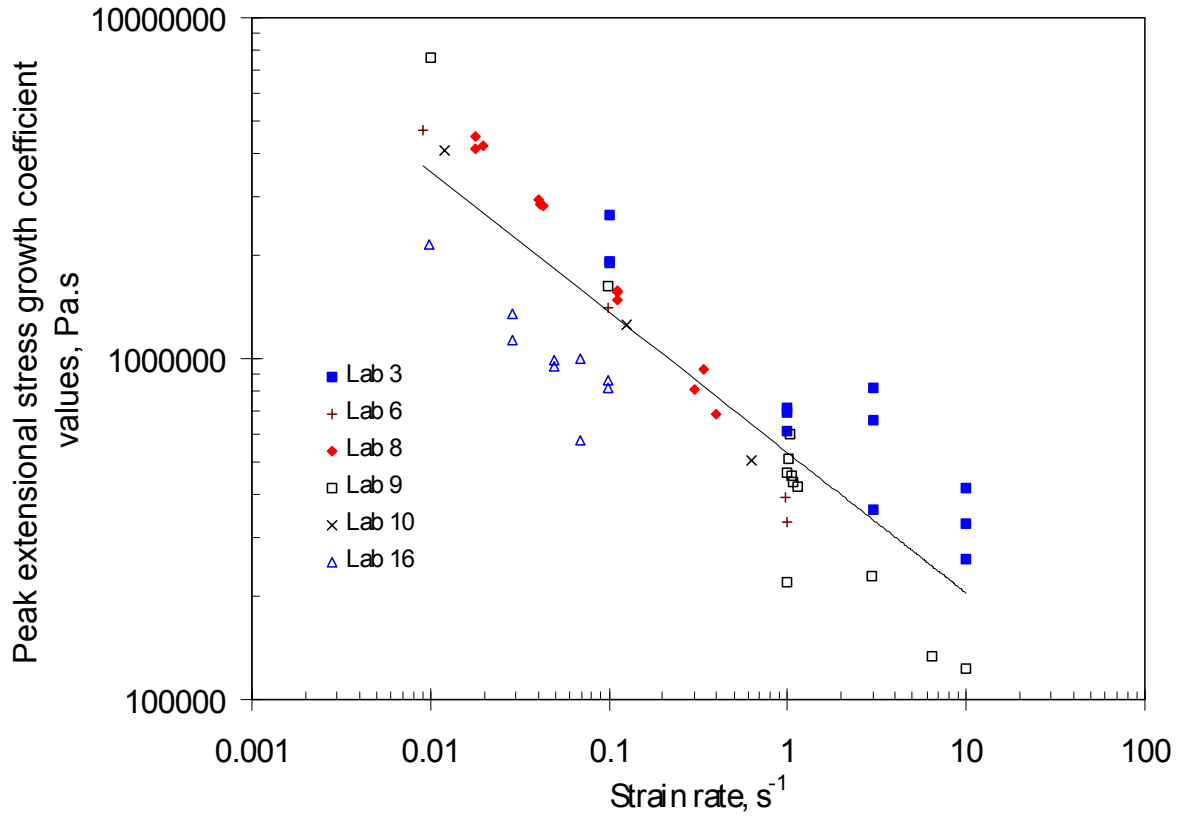

Figure 12 Comparison of peak extensional stress growth coefficient values obtained by all laboratories as a function of strain rate for a HDPE (HGH) at 150 ºC.

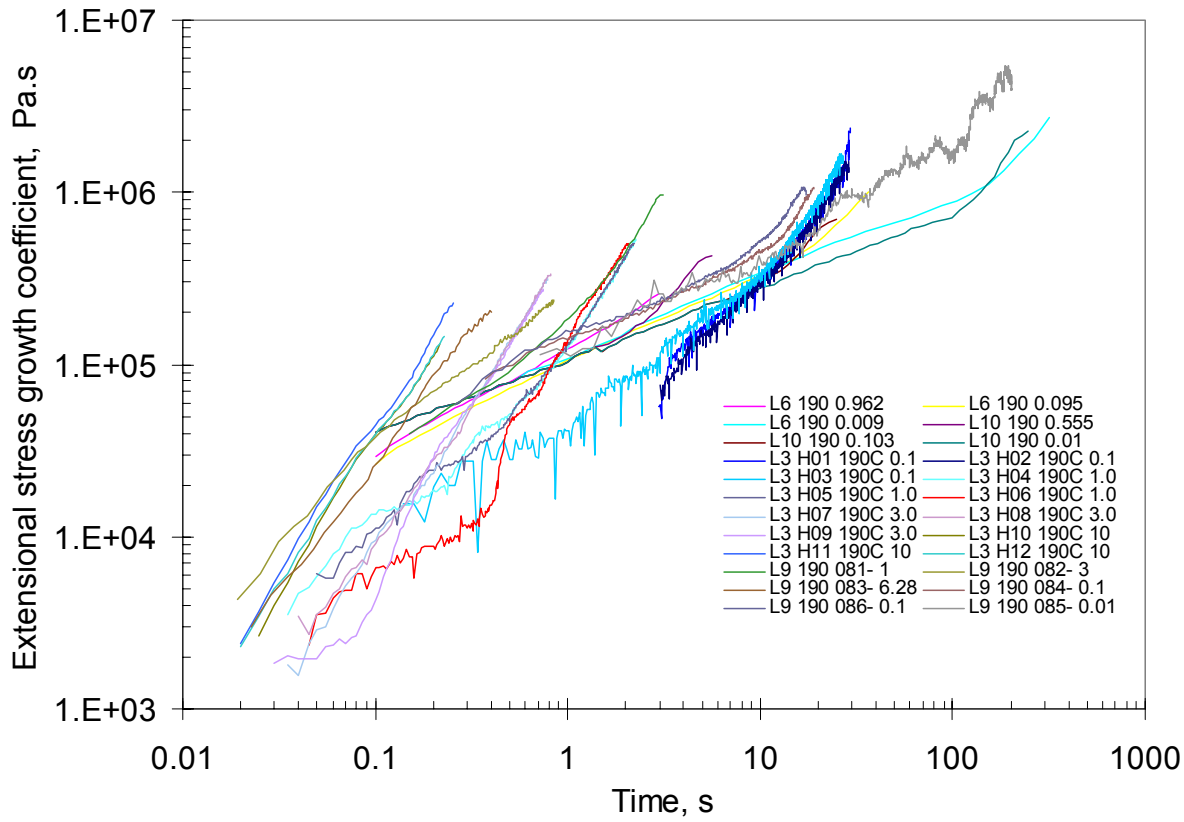

Figure 13 Intercomparison of stretching flow methods for a HDPE (HGH) at 190 ºC: all data.

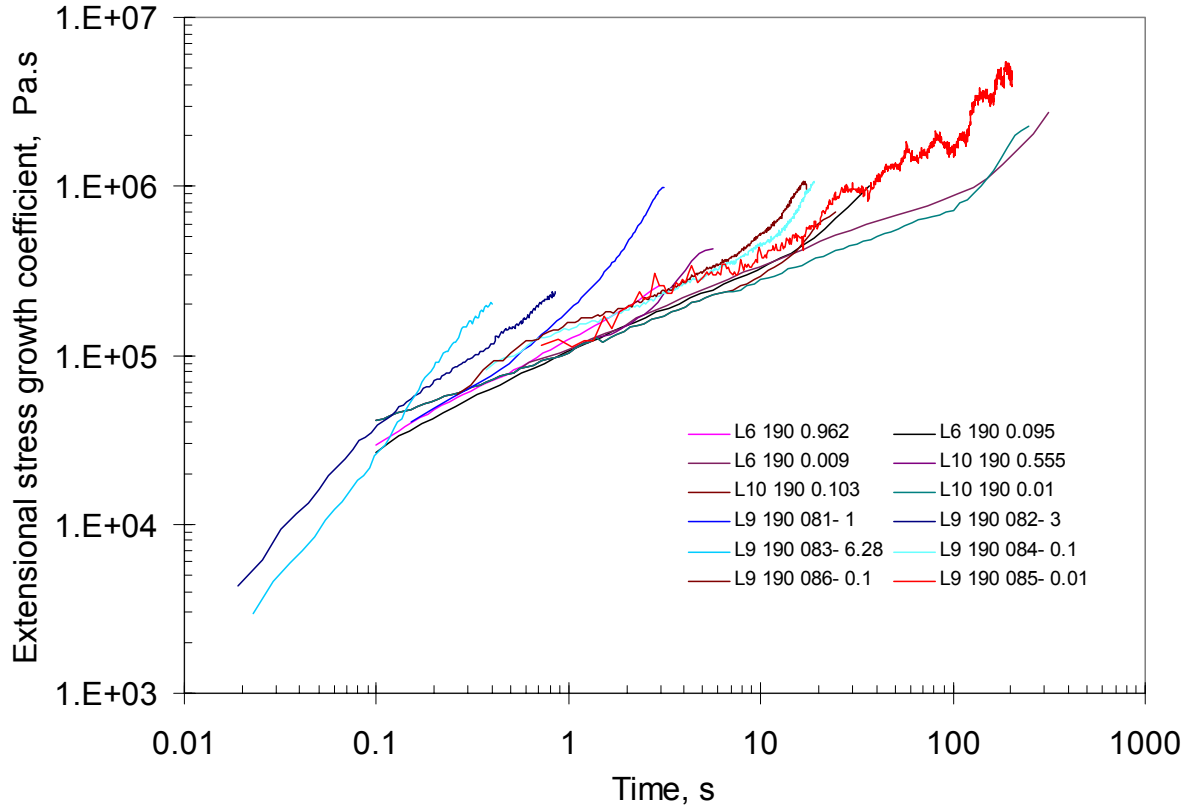

Figure 14 Intercomparison of stretching flow methods for a HDPE (HGH) at 190 ºC: laboratory 3 data removed.

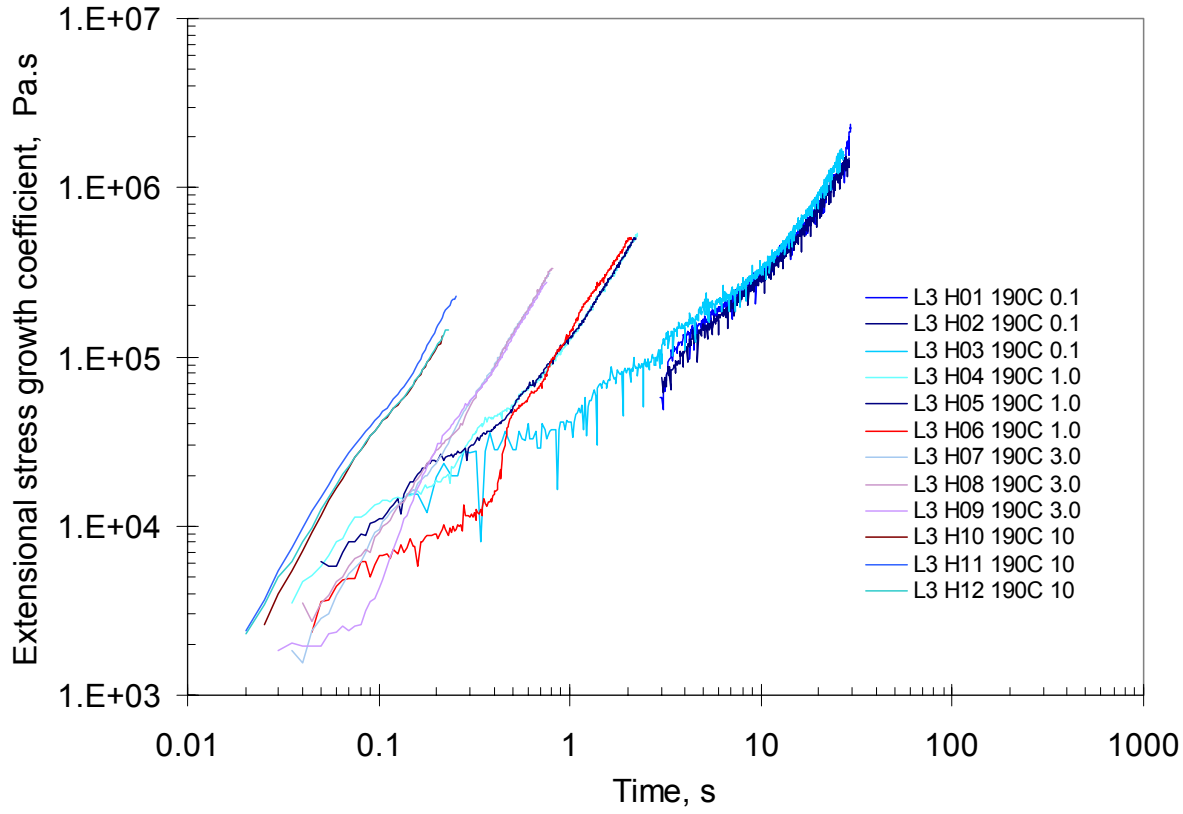

Figure 15 Extensional stress growth coefficient data for laboratory 3 for a HDPE (HGH) at 190 ºC.

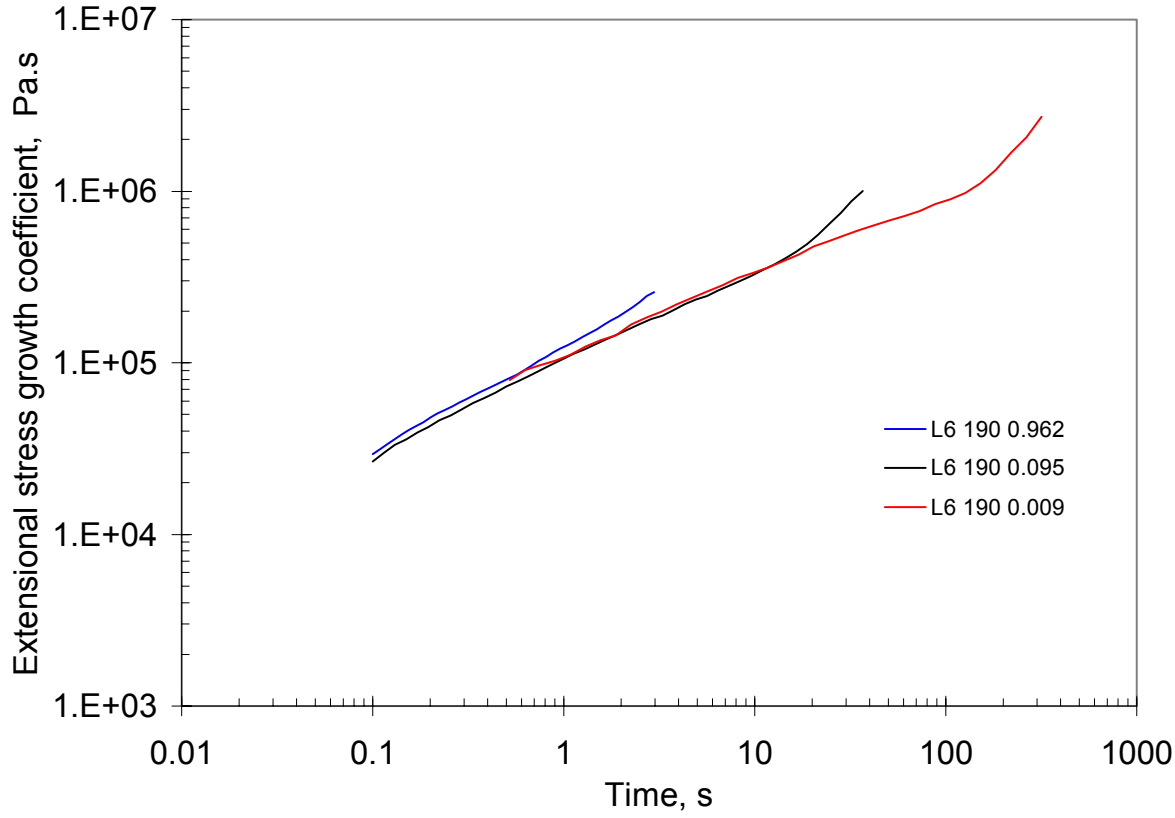

Figure 16 Extensional stress growth coefficient data for laboratory 6 for a HDPE (HGH) at 190 ºC.

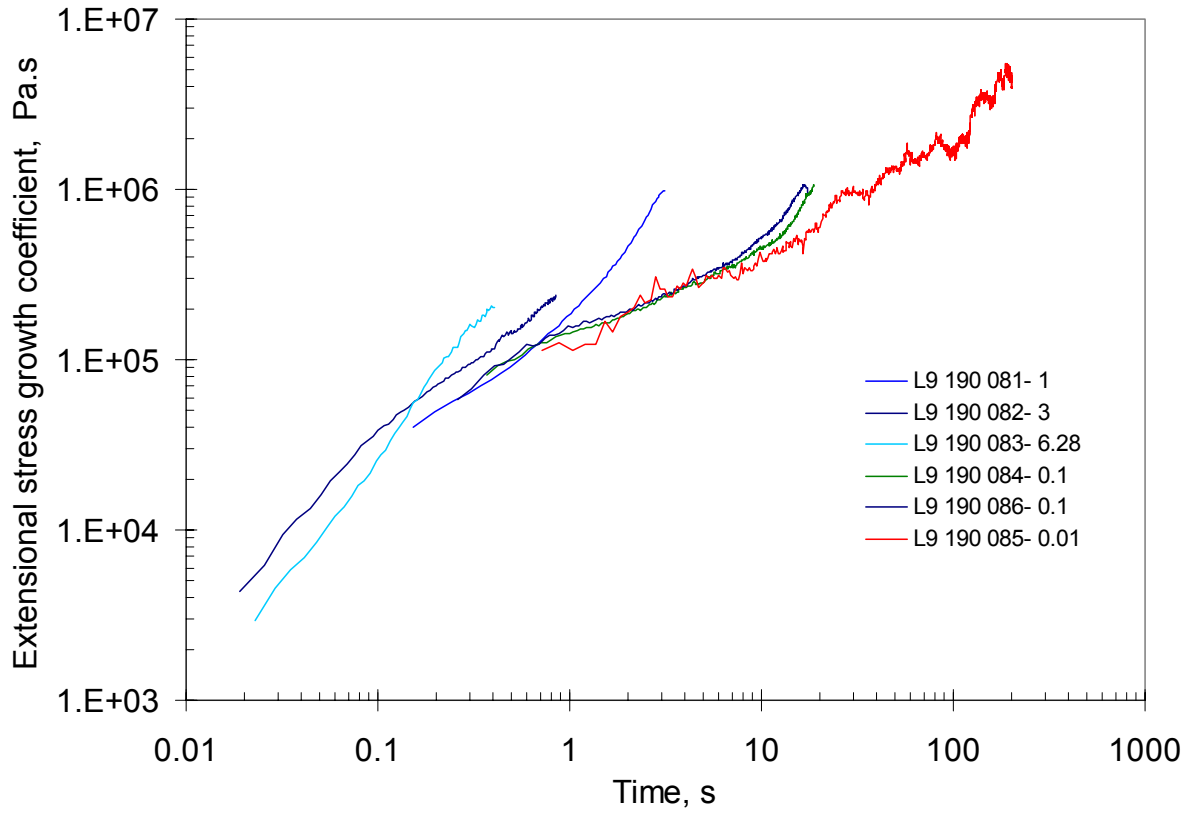

Figure 17 Extensional stress growth coefficient data for laboratory 9 for a HDPE (HGH) at 190 ºC.

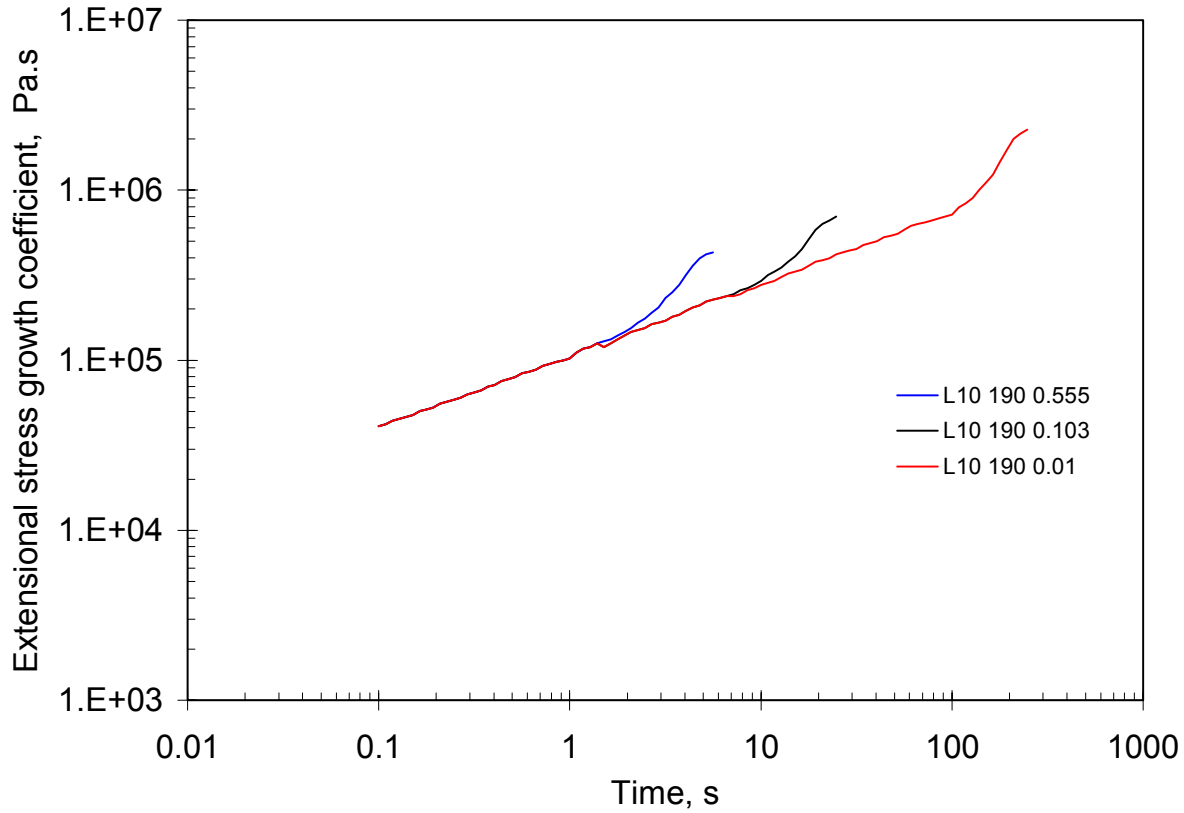

Figure 18 Extensional stress growth coefficient data for laboratory 10 for a HDPE (HGH) at 190 ºC.

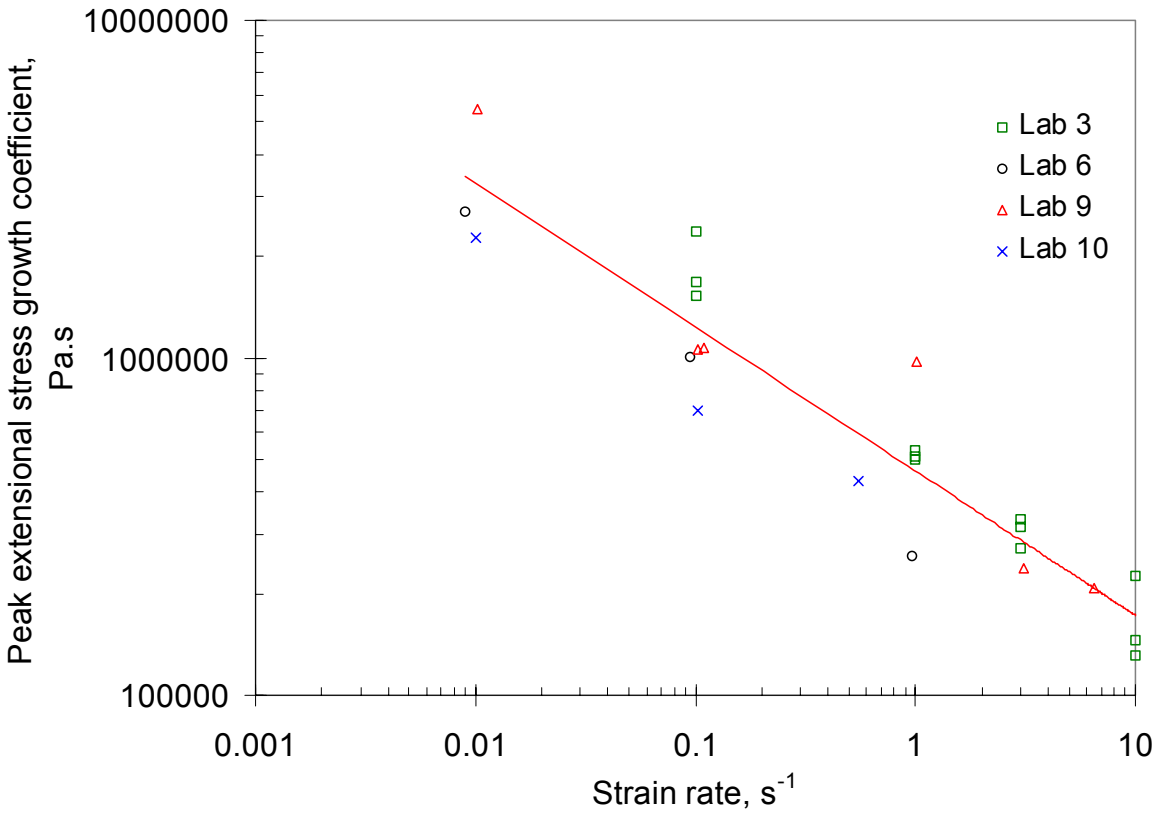

Figure 19 Comparison of peak extensional stress growth coefficient values obtained by all laboratories as a function of strain rate for a HDPE (HGH) at 190 ºC.

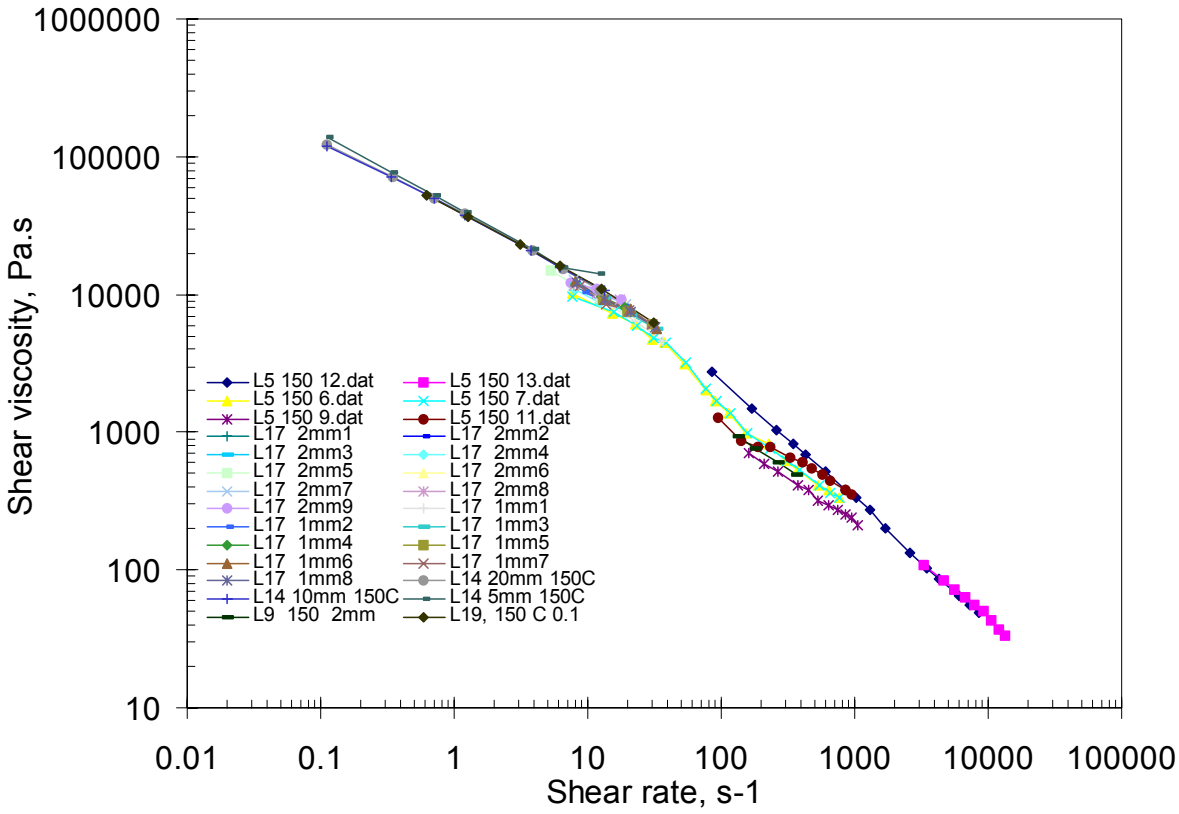

Figure 20 Shear viscosity data obtained by capillary extrusion rheometry for a HDPE (HGH) at 150 ºC.

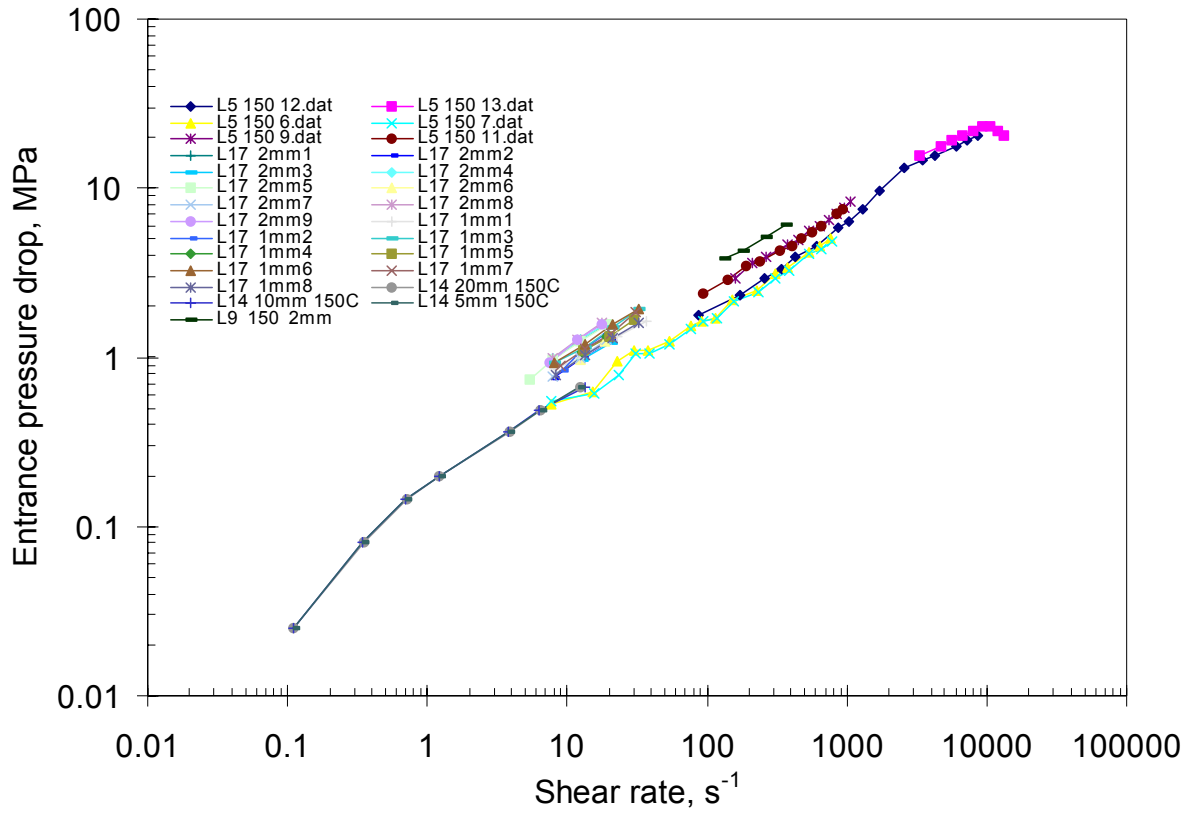

Figure 21 Entrance pressure drop data obtained by capillary extrusion rheometry for a HDPE (HGH) at 150 ºC.

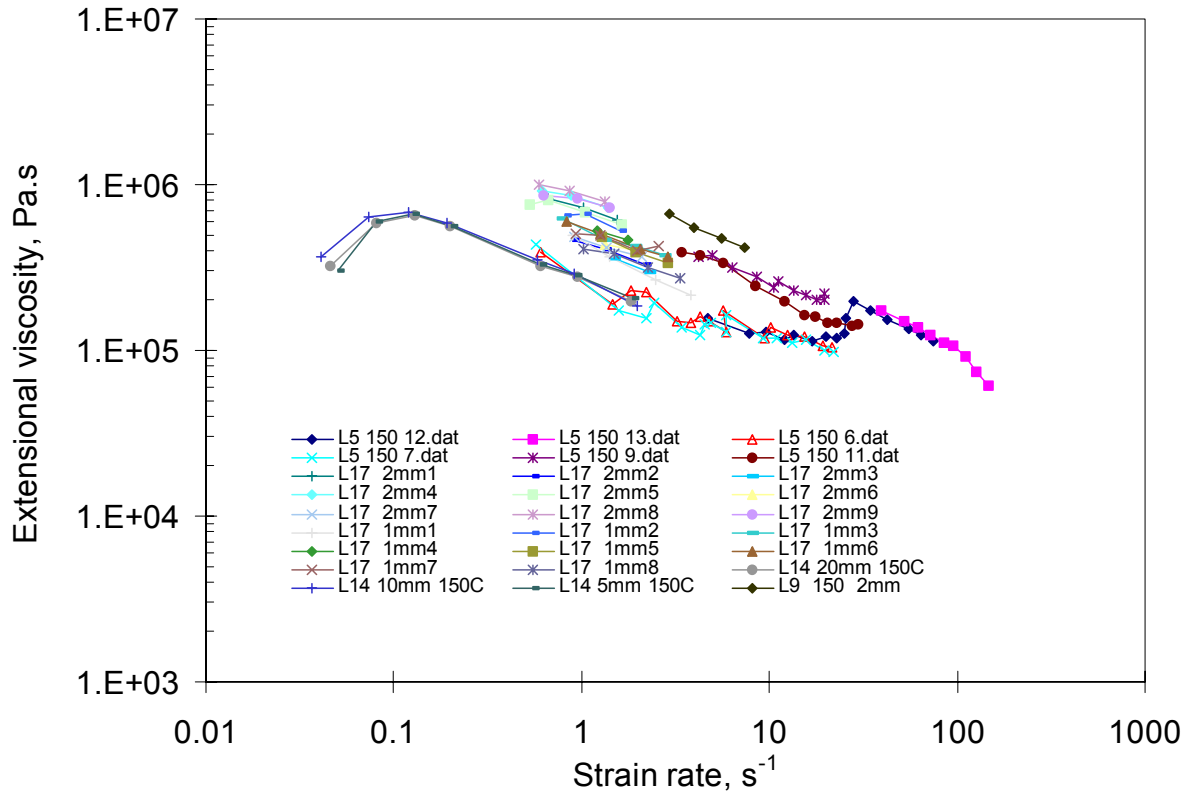

Figure 22 Extensional viscosity data obtained by interpretation of capillary extrusion rheometry entrance pressure drop data using the Cogswell model for a HDPE (HGH) at 150 ºC.

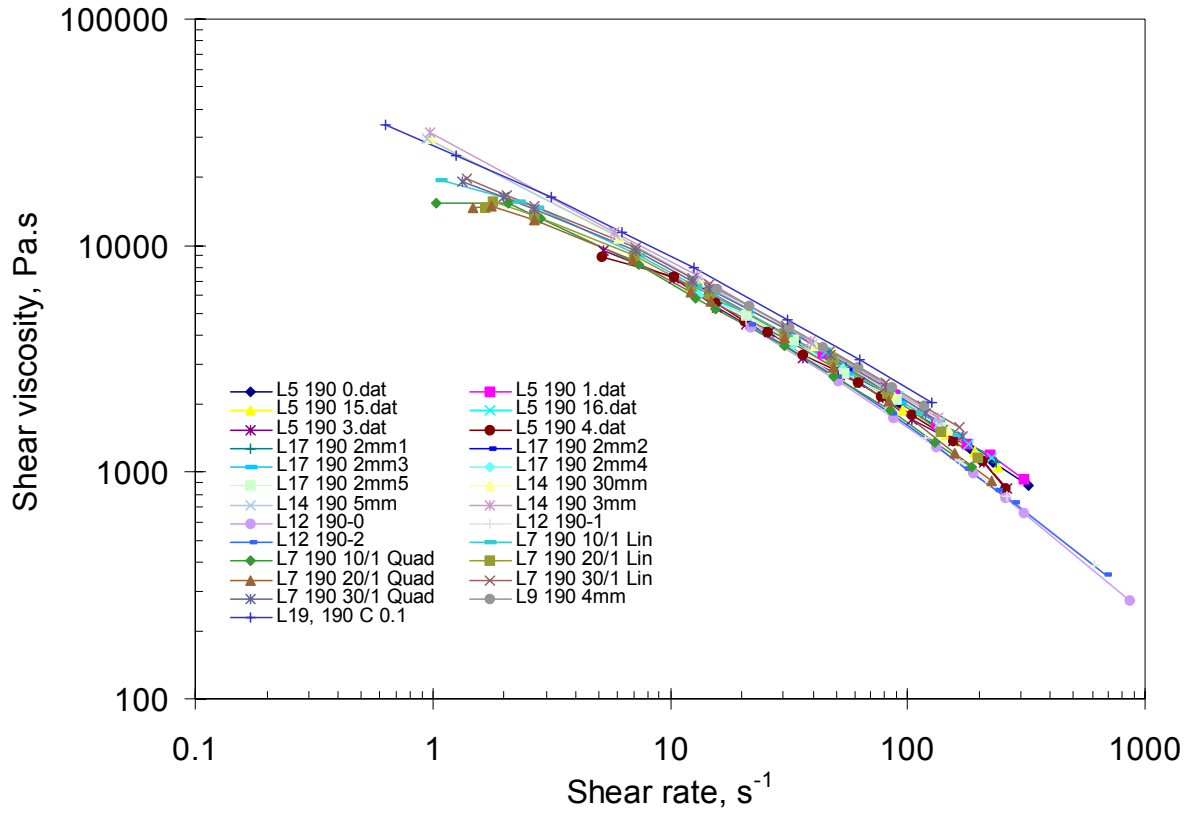

Figure 23 Shear viscosity data obtained by capillary extrusion rheometry for a HDPE (HGH) at 190 ºC.

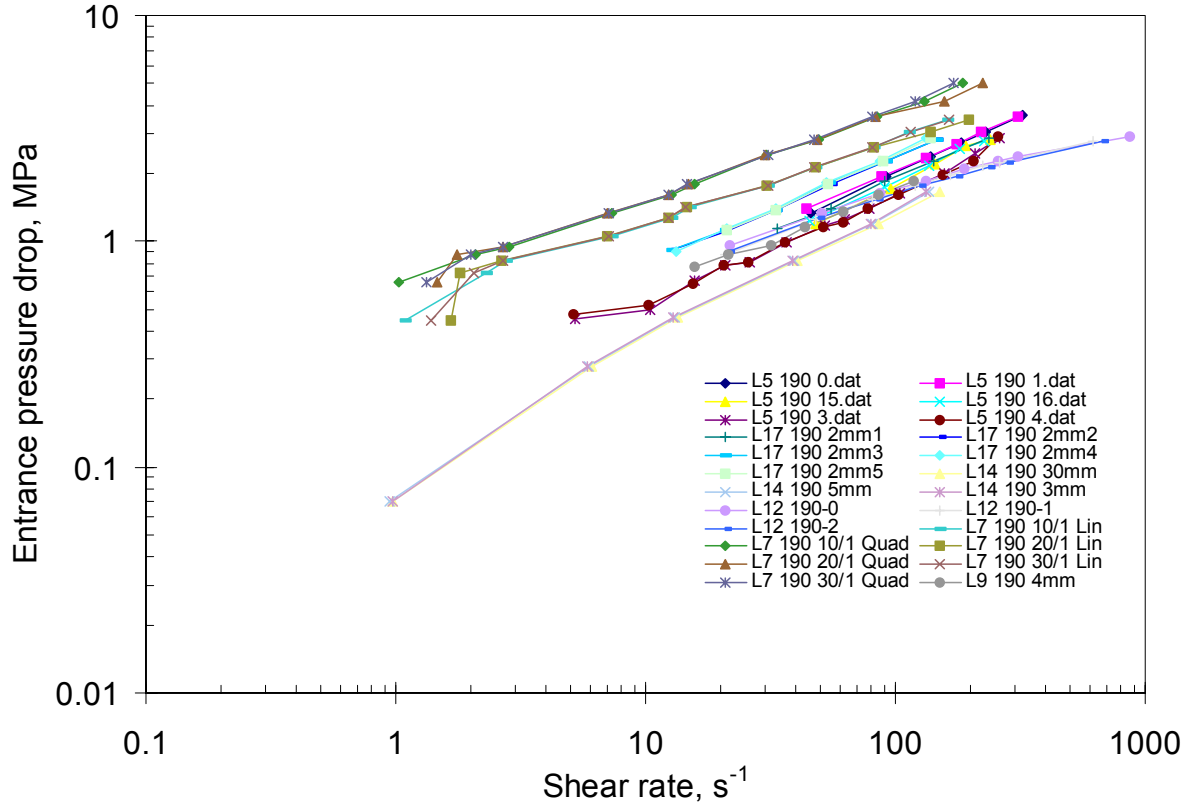

Figure 24 Entrance pressure drop data obtained by capillary extrusion rheometry for a HDPE (HGH) at 190 ºC.

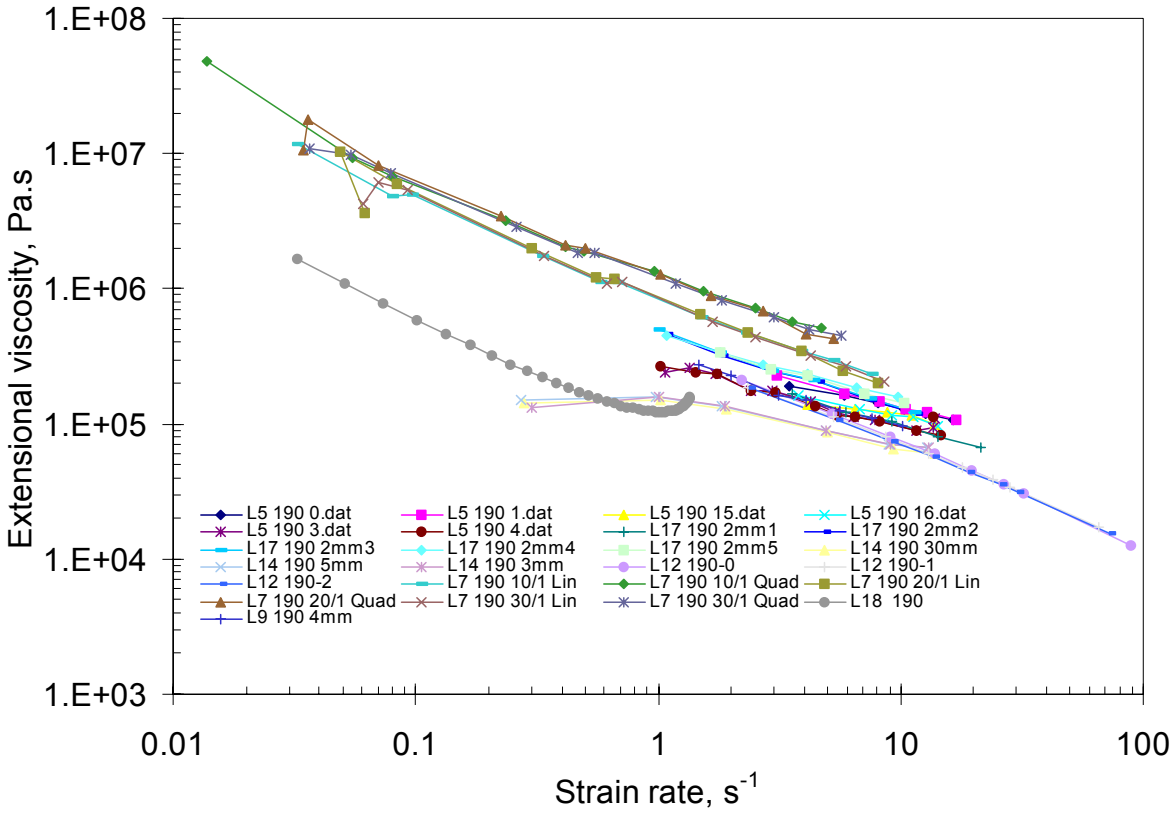

Figure 25 Extensional viscosity data obtained by interpretation of capillary extrusion rheometry entrance pressure drop data using the Cogswell model for a HDPE (HGH) at 190 ºC, and comparison with results obtained by visualisation of planar converging flow.

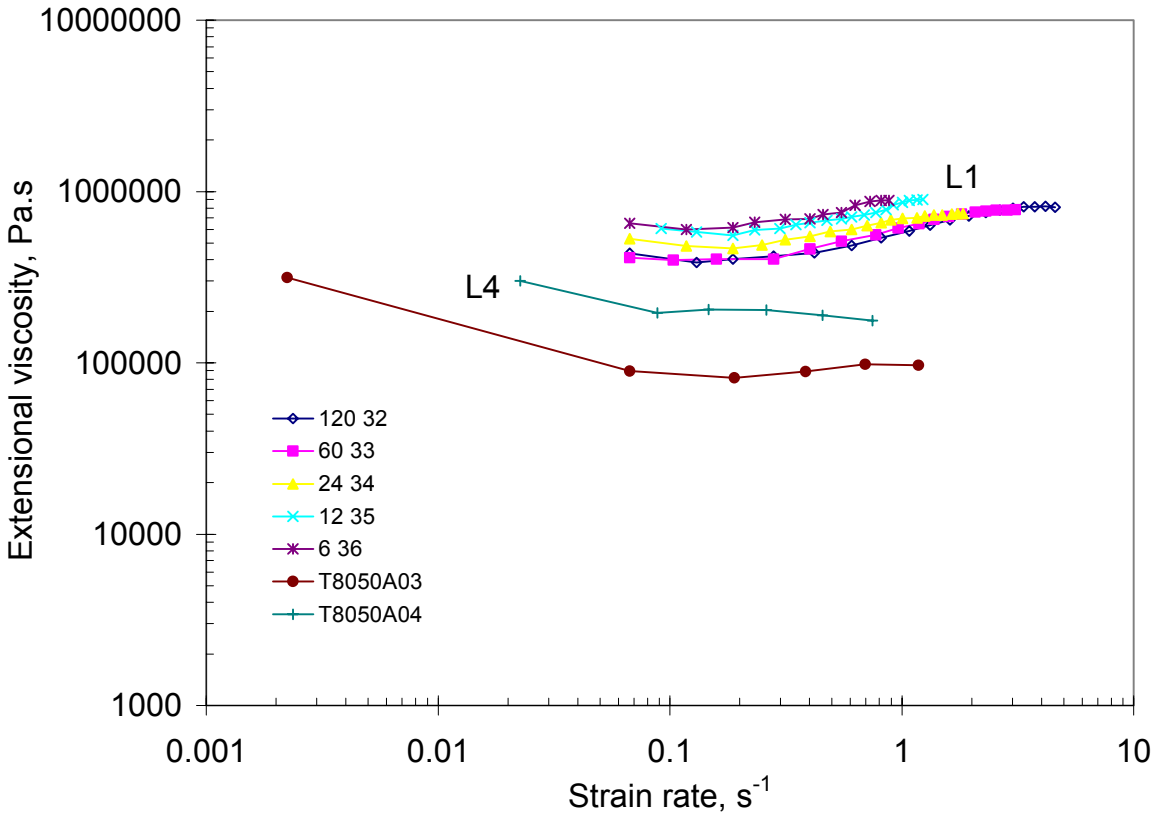

Figure 26 Extensional viscosity data as a functions of strain rate obtained by fibre spinning methods for a HDPE (HGH) at 190 ºC.

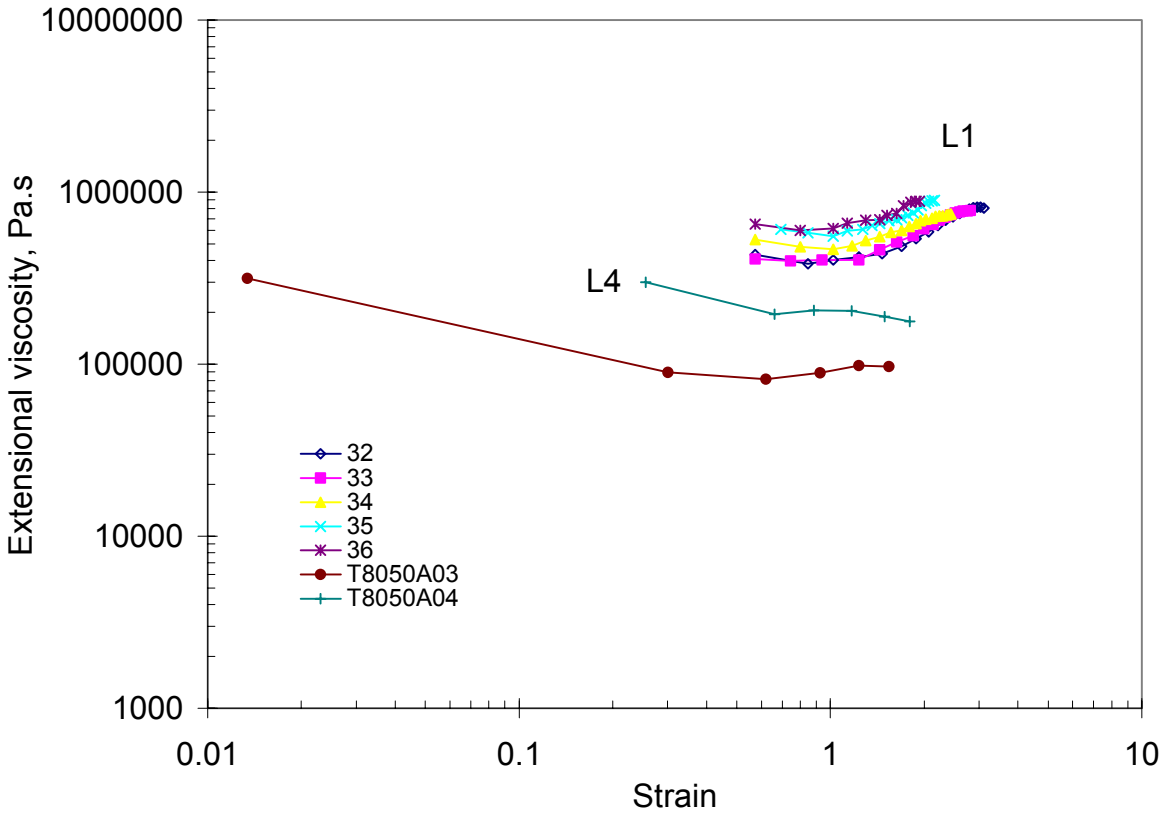

Figure 27 Extensional viscosity data as a functions of strain obtained by fibre spinning methods for a HDPE (HGH) at 190 ºC.

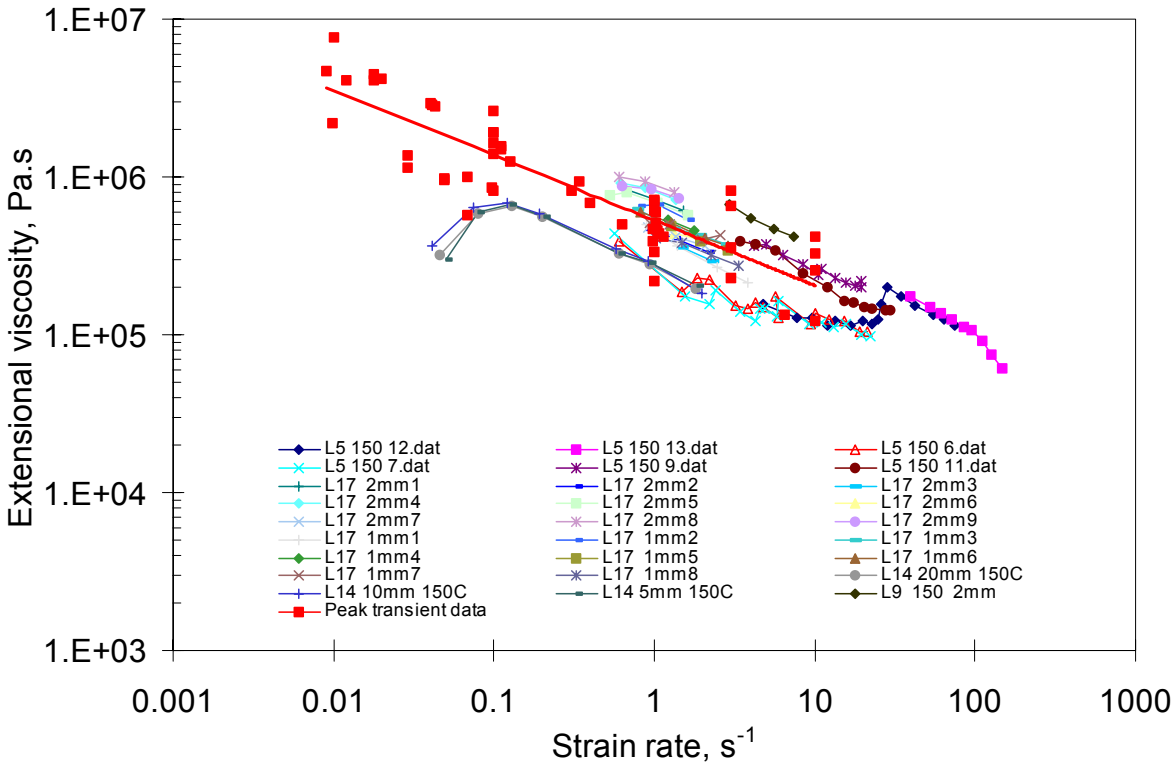

Figure 28 Comparison of peak transient extensional viscosity data obtained from stretching methods with "equilibrium" extensional viscosity data obtained using the Cogswell converging flow method for a HDPE (HGH) at 150 ºC.

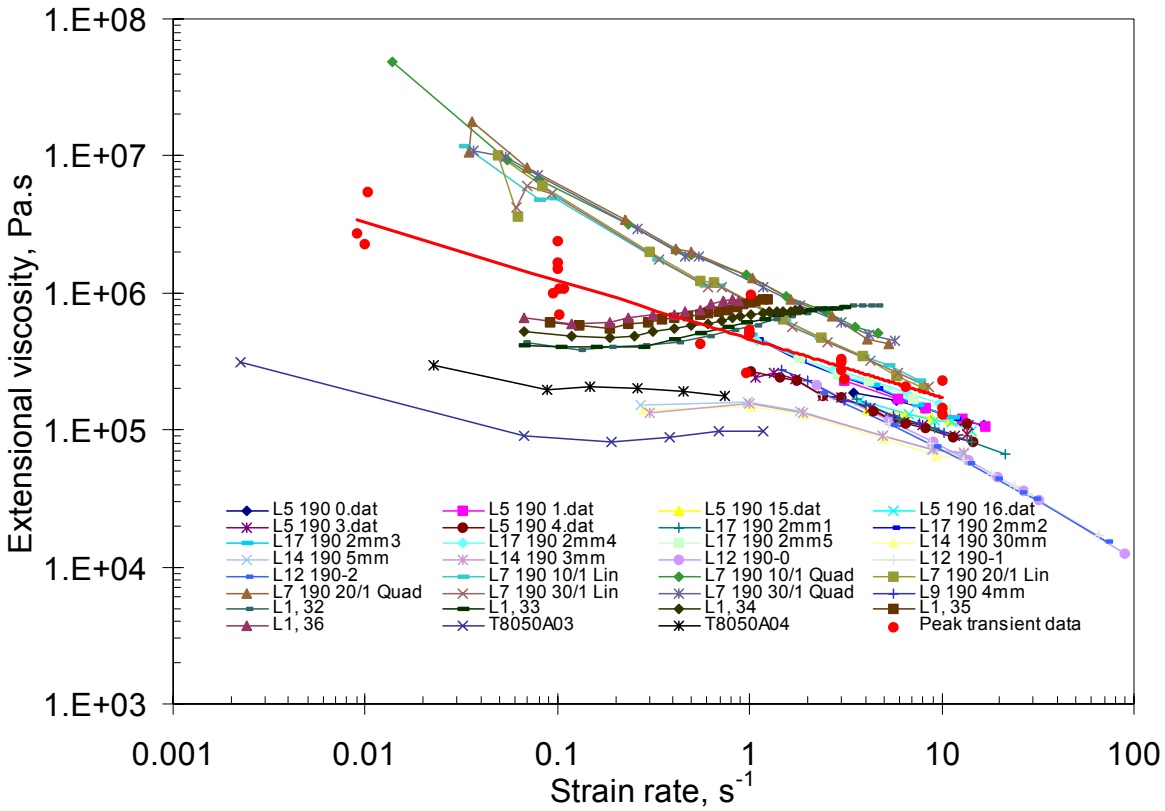

Figure 29 Comparison of peak transient extensional viscosity data obtained from stretching methods with "equilibrium" extensional viscosity data obtained using the Cogswell converging flow method and fibre spinning methods for a HDPE (HGH) at 190 ºC.

APPENDIX: DEFINITIONS OF STRAIN, STRAIN RATE, STRESS AND MATERIAL PROPERTIES FUNCTIONS IN TENSILE (SIMPLE) EXTENSION

A1 STRAIN AND STRAIN RATE

The following definitions are given by Whorlow [12] for strains and strain rates. Further descriptions are given by, for example, Gupta et al [8] and Dealy [9, 10].

A1.1 Elongation ratio

The *Elongation ratio (ER)* is the ratio of the current length ℓ to the initial length ℓ_o of the specimen:

$$ER = \ell / \ell_o.$$

A1.2 Hencky ε strains

The *Hencky strain* ε (also referred to as the natural or true strain) is given by the natural logarithm of the elongation ratio:

$$\varepsilon = \ln (\ell / \ell_o)$$

A1.3 Hencky $\dot{\varepsilon}$ strain rates

The *Hencky strain rate* is given by

$$\dot{\varepsilon} = 1/\ell \times \partial \ell / \partial t.$$

A2 MATERIAL PROPERTIES

Following the notation presented by Dealy [32] and prepared by the Nomenclature Committee of the Society of Rheology, for start-up flow in tensile (simple) extension at constant (Hencky) strain rate $\dot{\varepsilon}$ the following definitions are given. Equivalent expressions for cessation of steady tensile extension, tensile creep, tensile recoil and tensile step strain are presented by Dealy [32].

A2.1 Net tensile stress

The *net tensile stress* σ_E is defined by

$$\sigma_E = \sigma_{11} - \sigma_{22} = \sigma_{11} - \sigma_{33} = \sigma_{zz} - \sigma_{rr}$$

where σ_{ii} is a stress tensor in either rectangular or axisymmetric co-ordinates. The tensile stress growth function is indicated by σ_E^+ where the + indicates start-up rather than cessation of flow.

A2.2 Tensile stress growth coefficient

The *tensile stress growth coefficient* η_E^+ is defined by:

$$\eta_E^+(t, \dot{\varepsilon}) = \sigma_E / \dot{\varepsilon}$$

where t is time.

A2.3 Tensile viscosity

The *tensile viscosity* η_E is defined by:

$$\eta_E(t, \dot{\varepsilon}) = \lim_{t \to \infty} [\eta_E^+(t, \dot{\varepsilon})]$$

File ref.: CMMT(A)171 Extensional Intercomparison report_v#8_full version.doc, 6 April, 1999, 18:58